Pursuit Winning Strategies for Reach-Avoid Games with Polygonal Obstacles

Rui Yan, Shuai Mi, Xiaoming Duan, Jintao Chen, and Xiangyang Ji

Abstract—This paper studies a multiplayer reach-avoid differential game in the presence of general polygonal obstacles that block the players' motions. The pursuers cooperate to protect a convex region from the evaders who try to reach the region. We propose a multiplayer onsite and close-to-goal (MOCG) pursuit strategy that can tell and achieve an increasing lower bound on the number of guaranteed defeated evaders. This pursuit strategy fuses the subgame outcomes for multiple pursuers against one evader with hierarchical optimal task allocation in the receding-horizon manner. To determine the qualitative subgame outcomes that who is the game winner, we construct three pursuit winning regions and strategies under which the pursuers guarantee to win against the evader, regardless of the unknown evader strategy. First, we utilize the expanded Apollonius circles and propose the *onsite pursuit winning* that achieves the capture in finite time. Second, we introduce convex goal-covering polygons (GCPs) and propose the *close-to-goal pursuit winning* for the pursuers whose visibility region contains the whole protected region, and the goal-visible property will be preserved afterwards. Third, we employ Euclidean shortest paths (ESPs) and construct a pursuit winning region and strategy for the non-goal-visible pursuers, where the pursuers are firstly steered to positions with goal visibility along ESPs. In each horizon, the hierarchical optimal task allocation maximizes the number of defeated evaders and consists of four sequential matchings: capture, enhanced, non-dominated and closest matchings. Numerical examples are presented to illustrate the results.

Index Terms—Reach-avoid games, differential games, polygonal obstacles, pursuit winning, Euclidean shortest paths.

I. Introduction

Problem motivation and description: Differential games provide a proper mathematical framework to study the strategic behaviors of the players in the continuous state and action spaces [17]. We consider a multiplayer reach-avoid differential game in a polygonal region with general polygonal obstacles. In this game, multiple pursuers protect a convex region against a number of malicious evaders. However, the obstacles block the motion of all players. We propose a hierarchical-matching receding-horizon cooperative pursuit strategy that is computationally efficient and can achieve a continuously improving lower bound on the number of evaders that can be defeated. Our study is motivated by the recent popularity of reach-avoid differential games [6], [13], [22], [24], [29], [33], [36], [39],

R. Yan is with the Department of Computer Science, University of Oxford, Oxford, OX1 3QD, UK. {rui.yan@cs.ox.ac.uk}

S. Mi, J. Chen and X. Ji are with the Department of Automation, Tsinghua University, Beijing, 100084, China. {mis15@tsinghua.org.cn, cjt16@tsinghua.org.cn, xyji@tsinghua.edu.cn}

X. Duan is with the Department of Automation, Shanghai Jiao Tong University, Shanghai, 200240, China. {xduan@sjtu.edu.cn}

[40] and the lack of literature on efficient winning strategies for environments with obstacles.

Literature review: Reach-avoid differential games [24], [46], also known as two-target differential games [4], [14], perimeter defense games [33], or target guarding problems [11], [36], are a class of differential games in which the evaders (or attackers) attempt to reach a target set while avoiding the capture by the pursuers (or defenders). The prevalence of such games in the last decade is a result of pressing needs to provide intelligent strategies for protecting critical infrastructures such as buildings and airports, against malicious air drones and robots. There are four common approaches to address reach-avoid differential games. The classical Hamilton-Jacobi (HJ) analysis, provides a general methodology, applies to nonlinear dynamics and is ideal for low-dimensional systems [25], [26], [46]. The characteristic method, relying on integrating backward from non-unique terminal sets, can generate closed-form solutions if the underlying singular surfaces are identified properly [12], [36]. Computational geometry methods, utilising geometric concepts such as Voronoi diagram [47], Apollonius circle [27], [41], [44], function-based evasion space [40] and dominance region [28], have produced a diversity of strategies for simple-motion players. General forward reachable sets have also been applied to linear and nonlinear dynamics [15], [29]. Learning-based approaches have emerged recently and been proved to be empirically superior, but still require more future effort for performance guarantees [19], [31], [35].

Most of the works on reach-avoid differential games assume obstacle-free environments, that is, the players can move freely in the environment [7], [30], [33], [34], [36], [37], [39]–[43]. However, the addition of obstacles enables the study of more complex and realistic scenarios [18]. For example, robots need to reach a pre-specified region in the obstacle-rich environments while avoiding other non-cooperative robots or moving objects, such as in urban search and rescue scenarios. Such games can also provide a framework to study the territory defense problems in urban and forest conflicts [2], [4]. The air drones for package delivery must avoid the buildings, no-fly zones and other air drones, and reach the destinations safely.

Pursuit-evasion differential games in the presence of obstacles have been studied in the literature, where the capture is the unique competition goal. For example, Oyler *et al.* [28] provided the dominance region in the presence of a line segment or a triangle obstacle. Sometimes the obstacles generate both motion and visibility constraints while the pursuer's goal is to maintain the evader's visibility at all times [23], [48]. Zhou *et al.* [45] proved that three pursuers are sufficient and sometimes necessary to guarantee the capture of an equal-speed evader in

a bounded, two-dimensional arena with obstacles. The pursuer can learn and exploit the obstacle-avoidance mechanism of the evader to drive the latter to a trap position instead of capturing it [21]. As a popular tool to address the safety considerations, control barrier functions are integrated to ensure the safety of the pursuers or evaders against obstacles [18].

However, reach-avoid differential games with obstacles are more interesting but receive less attention due to the complexity. HJ methods [6] intrinsically can deal with general obstacle environments, but they require the state space discretization (thus suffer from loss of accuracy), and are limited to systems up to about five states in practice [5]. The same scalability issue exists when approximating the game as a finite-state model and then synthesizing the strategies using LTL algorithms [32]. Efficient algorithms have been proposed with restrictions, such as discrete-time dynamics and linear-quadratic approximations [1]. Motion planning approaches can be combined to generate obstacle-free paths when the pursuers instead guard the target by herding the evaders into a safe area [8].

Current approaches for reach-avoid differential games in the presence of obstacles suffer from at least one of the following drawbacks: the curse of dimensionality due to the state space discretization, heavy computational burden, model approximations and lack of winning guarantees (i.e., the construction of winning regions is missing). The winning regions [17], which are subsets of the state space, are very appealing and useful. A player can win if the game starts from a state in its own winning region, despite the opponent's strategy. As far as we know, although the winning regions for reach-avoid differential games without obstacles, have been treated in the literature [9], [13], [33], [39]–[43], an efficient approach for computing winning regions and strategies for environments with obstacles is missing, and it becomes even harder for multiplayer games.

Contributions: Utilising computational geometry methods and the hierarchical matching, we propose a multiplayer onsite and close-to-goal (MOCG) pursuit strategy for reach-avoid differential games in the presence of general polygonal obstacles. This strategy is computed efficiently, and can provide and achieve a lower bound on the number of defeated evaders that continuously improves over time. The main contributions are as follows:

1) For the subgame with multiple pursuers and one evader, we propose three pairs of pursuit winning regions and the corresponding strategies that guarantee the winning of pursuers: *onsite pursuit winning*, goal-visible and non-goal-visible cases for *close-to-goal pursuit winning*. All results apply to the bounded polygonal environments with general polygonal obstacles.

2) For the onsite pursuit winning, we propose a multiplayer pursuit strategy based on expanded Apollonius circles in [9], and then construct the related winning region. In this winning, the pursuers can guarantee to capture the evader in an obstacle-free area and in finite time, targeting scenarios where players are close to each other with no obstacles nearby.

3) For the close-to-goal pursuit winning, if the pursuers are goal-visible, i.e., all points in the goal region are visible to the pursuers, we introduce convex goal-covering poly-

gons (GCPs). We then propose a GCP-based multiplayer pursuit strategy and construct the related winning region. This strategy ensures that pursuers are goal-visible at all times. In this winning, at most two pursuers are needed.

4) For the close-to-goal pursuit winning, if a pursuer is not goal-visible, we combine GCPs with Euclidean shortest path and propose a two-stage pursuit strategy. Then, we construct the related winning region based on the convex optimization. In this winning, the game will evolve to one of last two cases eventually.

5) Finally, we present a hierarchical task assignment scheme to merge all these subgame outcomes. A receding-horizon MOCG pursuit strategy is proposed such that the number of guaranteed defeated evaders is maximized at each step and increases with iterations.

Paper organization: We introduce reach-avoid differential games with polygonal obstacles in Section II. We present the onsite pursuit winning, the goal-visible and non-goal-visible cases for close-to-goal pursuit winning in Sections III, IV and V, respectively. In Section VI, we propose the MOCG pursuit strategy. Numerical results are presented in Section VII and we conclude the paper in Section VIII.

Notation: Let $\mathbb{R}$ be the set of reals. Let $\mathbb{R}^n$ be the set of n-dimensional real column vectors and $\|\cdot\|_2$ be the Euclidean norm. Let $\boldsymbol{x}^\top$ denote the transpose of a vector $\boldsymbol{x} \in \mathbb{R}^n$. Denote the unit disk in $\mathbb{R}^n$ by $\mathbb{S}^n$, i.e., $\mathbb{S}^n = \{\boldsymbol{u} \in \mathbb{R}^n \mid \|\boldsymbol{u}\|_2 \le 1\}$. For a finite set S, let $|S|$ be the cardinality of S. All angles in this paper are in the range $[0, 2\pi)$. For two angles θ_1 and θ_2, let $D[\theta_1, \theta_2]$ be the set of angles from θ_1 to θ_2 in a counter-clockwise direction, and $|D[\theta_1, \theta_2]|$ be the corresponding angle difference from θ_1 to θ_2, also called angle span of $D[\theta_1, \theta_2]$. For two points $\boldsymbol{x}_1, \boldsymbol{x}_2 \in \mathbb{R}^2$, let $\overline{\boldsymbol{x}_1 \boldsymbol{x}_2}$ be the line segment with endpoints $\boldsymbol{x}_1$ and $\boldsymbol{x}_2$, and $\sigma(\boldsymbol{x}_1, \boldsymbol{x}_2)$ be the angle of the vector from $\boldsymbol{x}_1$ to $\boldsymbol{x}_2$. For three distinct points $\boldsymbol{x}_1, \boldsymbol{x}_2, \boldsymbol{x}_3 \in \mathbb{R}^2$, let $\mathcal{R}_{\mathrm{tri}}(\boldsymbol{x}_1, \boldsymbol{x}_2, \boldsymbol{x}_3) \subset \mathbb{R}^2$ be the triangle region with vertices $\boldsymbol{x}_1, \boldsymbol{x}_2$ and $\boldsymbol{x}_3$, and $\mathcal{R}_{\mathrm{sec}}(\boldsymbol{x}_1, \boldsymbol{x}_2, \boldsymbol{x}_3) \subset \mathbb{R}^2$ be the unbounded circular sector by counterclockwise sweeping the line emanating from $\boldsymbol{x}_1$ to $\boldsymbol{x}_2$ until the line from $\boldsymbol{x}_1$ to $\boldsymbol{x}_3$. Further notations are provided in Table I, which will be explained in more detail later.

II. PROBLEM STATEMENT

A. Reach-avoid differential games with polygonal obstacles

Consider a planar reach-avoid differential game in a polygonal region $\Omega \subset \mathbb{R}^2$ with N_p pursuers, $\mathscr{P} = \{P_1, \dots, P_{N_p}\}$, and N_e evaders, $\mathscr{E} = \{E_1, \dots, E_{N_e}\}$, as depicted in Fig. 1. Each player is assumed to be a mass point and moves with simple motion as Isaacs states [17], i.e., it is holonomic. The dynamics of the players are described by

$$\begin{aligned} \dot{\boldsymbol{x}}_{P_i}(t) &= v_{P_i} \boldsymbol{u}_{P_i}(t), & \boldsymbol{x}_{P_i}(0) &= \boldsymbol{x}_{P_i}^0, & P_i &\in \mathscr{P} \\ \dot{\boldsymbol{x}}_{E_j}(t) &= v_{E_j} \boldsymbol{u}_{E_j}(t), & \boldsymbol{x}_{E_j}(0) &= \boldsymbol{x}_{E_j}^0, & E_j &\in \mathscr{E} \end{aligned} \quad (1)$$

where $\boldsymbol{x}_{P_i} \in \mathbb{R}^2$ and $\boldsymbol{x}_{E_j} \in \mathbb{R}^2$ are the positions of P_i and E_j, respectively, and $\boldsymbol{u}_{P_i}$ and $\boldsymbol{u}_{E_j}$ are their control inputs that belong to the admissible control set $\mathbb{U} = \{\boldsymbol{u} : [0, \infty) \to \mathbb{S}^2 \mid \boldsymbol{u}$ is piecewise smooth$\}$. For P_i and E_j, their maximum

Table 1. Notation Table

Symbol	Description	Symbol	Description
$\mathscr{P}$	N_p pursuers $\{P_1, \ldots, P_{N_p}\}$	$\mathscr{E}$	N_e evaders $\{E_1, \ldots, E_{N_e}\}$
$\mathcal{O}$	family of obstacles $\{O_1, \ldots, O_k\}$	$\Omega, \Omega_{\text{goal}}$	game region, convex goal region
Ω_{play}	play region $\Omega \setminus (\cup_{O \in \mathcal{O}} O \cup \Omega_{\text{goal}})$	Ω_{free}	$\Omega_{\text{play}} \cup \Omega_{\text{goal}}$ where players can move freely
$\alpha_{ij} = v_{P_i}/v_{E_j}$	speed ratio between P_i and E_j	r_i	capture radius of P_i
P_c	pursuit coalition $\{P_i \in \mathscr{P} \mid i \in c\}$	$X_c = \{\boldsymbol{x}_{P_i}\}_{i \in c}$	positions of all pursuers in coalition P_c
$X_{ij} = (\boldsymbol{x}_{P_i}, \boldsymbol{x}_{E_j})$	state of the subgame between P_i and E_j	$X_{cj} = (X_c, \boldsymbol{x}_{E_j})$	state of the subgame between coalition P_c and E_j
$\mathbb{A}$	Apollonius circle and its interior	$\mathbb{A}_\delta$	expanded Apollonius circle and its interior
$D_{\mathcal{R}}(\boldsymbol{x}) \in [0, 2\pi)$	direction range of $\boldsymbol{x}$ in $\mathcal{R}$	$\varrho(X_{cj})$	safe distance of the subgame between P_c and E_j
$P_{\text{ESP}}(\boldsymbol{x}_1, \boldsymbol{x}_2)$	Euclidean shortest path (ESP) between $\boldsymbol{x}_1$ and $\boldsymbol{x}_2$	$d_{\text{ESP}}(\boldsymbol{x}_1, \boldsymbol{x}_2)$	ESP distance between $\boldsymbol{x}_1$ and $\boldsymbol{x}_2$
$\mathcal{R}_{\text{ESP}}(\boldsymbol{x}, \ell)$	ESP reachable region from $\boldsymbol{x}$ within distance ℓ	$W_{\text{ESP}}(\boldsymbol{x}, \ell)$	wavefront from $\boldsymbol{x}$ with distance ℓ

speeds are $v_{P_i} > 0$ and $v_{E_j} > 0$, respectively, and their initial positions are $\boldsymbol{x}_{P_i}^0 \in \mathbb{R}^2$ and $\boldsymbol{x}_{E_j}^0 \in \mathbb{R}^2$, respectively.

A family of obstacles in Ω, denoted by $\mathcal{O} = \{O_1, \ldots, O_k\}$, block the motions of the players, where each obstacle $O_i \subset \Omega$ ($1 \le i \le k$) is a simple polygon (all boundaries are excluded) and the closures of any two obstacles are disjoint. A *convex* polygon Ω_{goal} in Ω, which is disjoint from all obstacles and the pursuers and the evaders compete for, is called *goal region* (the green polygon in Fig. 1). Formally, we have $\Omega_{\text{goal}} = \{\boldsymbol{x} \in \mathbb{R}^2 \mid A_i \boldsymbol{x} + \boldsymbol{b}_i \ge 0, i \in I_{\text{goal}}\}$, where $A_i \in \mathbb{R}^{2 \times 2}, \boldsymbol{b}_i \in \mathbb{R}^2$ and I_{goal} is an index set. The game region Ω minus all obstacle polygons and the goal region is called *play region* and denoted by Ω_{play}, i.e., $\Omega_{\text{play}} = \Omega \setminus (\cup_{O \in \mathcal{O}} O \cup \Omega_{\text{goal}})$. We denote by $\Omega_{\text{free}} := \Omega_{\text{play}} \cup \Omega_{\text{goal}}$ the union of the play region and the goal region, in which all players can move freely.

We denote by $\alpha_{ij} = v_{P_i}/v_{E_j}$ the speed ratio between P_i and E_j and consider faster pursuers, i.e., $\alpha_{ij} > 1$. Let $r_i \ge 0$ be the capture radius of P_i. An evader is *captured* by P_i if P_i is pursuing the evader, their Euclidean distance is less than or equal to r_i and the line segment connecting them is obstacle-free (i.e., visual radius capture).

The evasion team $\mathscr{E}$ aims to send as many evaders initially in the play region Ω_{play} as possible into the goal region Ω_{goal} via the paths in Ω_{free}, before being captured by the pursuit team $\mathscr{P}$ which conversely strives to guard Ω_{goal} against $\mathscr{E}$.

In this problem, we consider the state feedback information structure [3]. The pursuit and evasion teams make decisions about their current control inputs with the information of all players' current positions. The maximum speeds of all players, the capture radii of all pursuers and the information about Ω, Ω_{play}, Ω_{goal} and $\mathcal{O}$ are known by two teams.

B. Multiple-pursuer-one-evader subgames

There exists complex, non-intuitive cooperation among team members and competition among players from different teams. Thus, it is challenging to synthesize strategies for multiple pursuers and multiple evaders directly. We split the whole game into many subgames, compute strategies for each subgame separately and generate team strategies by piecing together all subgame outcomes. This approach has been widely used to solve multiplayer games [6], [13], [33], [39], [40]. Notably, the very relevant work [6] by Chen et al. only considered one-pursuer-one-evader subgames and solved multiplayer games
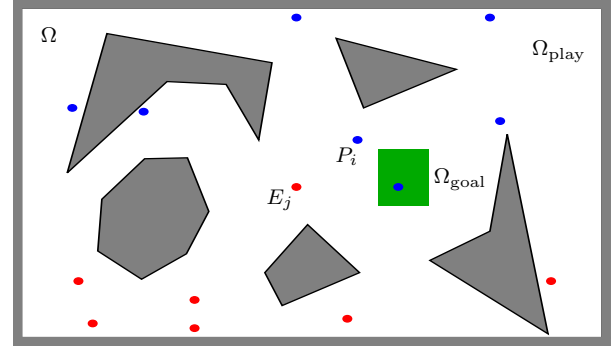

Fig. 1. Multiplayer reach-avoid differential games in the presence of black general polygonal obstacles, where the blue pursuers protect a green convex polygon Ω_{goal} against the red evaders who start from the play region Ω_{play} and aim to enter Ω_{goal}. The obstacles block the motion of all players.

by fusing pairwise outcomes via the maximum matching. In this paper, we consider the subgames with multiple pursuers and one evader and fuse the subgame outcomes via hierarchical optimal task allocation.

We introduce several definitions and notations for a set of pursuers. For any non-empty index set $c \in 2^{\{1,\ldots,N_p\}}$, let $P_c = \{P_i \in \mathscr{P} \mid i \in c\}$ be a *pursuit coalition* containing pursuer P_i if $i \in c$. We denote by X_c and U_c the positions and the control inputs of all pursuers in P_c, respectively, i.e., $X_c = \{\boldsymbol{x}_{P_i}\}_{i \in c}$ and $U_c = \{\boldsymbol{u}_{P_i}\}_{i \in c}$. Let the product of $|c|$ sets $\mathbb{U}$, i.e., $\mathbb{U}_c = \mathbb{U} \times \cdots \times \mathbb{U}$, be the admissible control set for P_c. Let $X_{cj} = (X_c, \boldsymbol{x}_{E_j})$ be the state (i.e., position) of the subgame between P_c and E_j, and $X_{ij} = (\boldsymbol{x}_{P_i}, \boldsymbol{x}_{E_j})$ be the subgame state (i.e., position) if $c = \{i\}$. Any variable that depends on the players' positions $\boldsymbol{x}_{P_i}(t)$ or $\boldsymbol{x}_{E_j}(t)$ is time-dependent. For notational convenience, we omit t unless needed for clarity.

For a subgame between a pursuit coalition P_c and an evader E_j, the pursuit winning is defined as follows.

Definition 1 (Pursuit winning). *A pursuit coalition $P_c \in 2^{\mathscr{P}}$ guarantees to win against an evader $E_j \in \mathscr{E}$ at a state X_{cj}, if there exists a pursuit strategy $U_c \in \mathbb{U}_c$ such that starting from X_{cj}, one of the conditions holds regardless of E_j's strategy:*

1) P_c can guarantee to capture E_j in Ω_{play};

2) P_c can guarantee to delay E_j from entering Ω_{goal} forever unless E_j is captured.

The state X_{cj} and the strategy U_c are called a pursuit winning state and a corresponding winning strategy, respectively. A set of pursuit winning states are called a pursuit winning region.

C. Problems of interest

In this paper, our goal is to propose strategies for the pursuit team $\mathscr{P}$ that can guarantee to win against as many evaders simultaneously as possible (i.e., capture evaders or delay them from entering Ω_{goal} forever). The idea is to divide the pursuers into many disjoint coalitions and then assign each coalition with a carefully designed pursuit strategy to a particular evader.

To this end, we first construct three pursuit winning regions (i.e., positions of a pursuit coalition and an evader) from which the pursuit coalition can win regardless of the evader's strategy. These three pursuit winning regions correspond to different scenarios informally defined as follows and detailed later.

Definition 2 (Three pursuit winning regions). *For a pursuit coalition and an evader, an* onsite *pursuit winning region corresponds to the scenario where the pursuers are close to the evader with no obstacles nearby. The goal-visible case for the* close-to-goal *pursuit winning region corresponds to the scenario where the pursuers can visibly see the whole goal region, while the non-goal-visible case corresponds to the scenario where the visibility is not satisfied.*

Then, three pursuit winning regions are used during the play to determine whether a pursuit coalition can win against an evader. By collecting all such subgame outcomes, we generate disjoint pursuit coalitions and assign them to evaders in real time such that the number of defeated evaders is maximized, where each pursuit coalition will either take the strategy that ensures its winning or some heuristic strategy detailed below. The assignment will change if a new assignment guaranteeing to defeat more evaders is generated as the game evolves.

III. ONSITE PURSUIT WINNING

For a subgame between a pursuit coalition P_c and an evader E_j, this section focuses on the onsite pursuit winning where E_j can be captured before the obstacles are used to assist its evasion. We present the pursuit winning region and the related winning strategy for P_c.

A. Expanded Apollonius-circle based pursuit strategy

We first recall an expanded Apollonius circle based pursuit strategy in the *obstacle-free* plane for one pursuer against one evader due to Dorothy et al. [9]. For a state X_{ij}, we define two variables:

$$R_A = \frac{\alpha_{ij} \| \boldsymbol{x}_{P_i} - \boldsymbol{x}_{E_j} \|_2}{\alpha_{ij}^2 - 1}, \ \boldsymbol{x}_A = \frac{\alpha_{ij}^2 \boldsymbol{x}_{E_j} - \boldsymbol{x}_{P_i}}{\alpha_{ij}^2 - 1}. \quad (2)$$

Then, the Apollonius circle [17] and its interior, denoted by $\mathbb{A}$, and its expanded version with a small constant $\delta > 0$, denoted by $\mathbb{A}_\delta$ (with the green boundary in Fig. 2(a)), are respectively computed as follows:

$$\begin{aligned} \mathbb{A} &= \{ \boldsymbol{x} \in \mathbb{R}^2 \mid \| \boldsymbol{x} - \boldsymbol{x}_A \|_2 \le R_A \}, \\ \mathbb{A}_\delta &= \{ \boldsymbol{x} \in \mathbb{R}^2 \mid \| \boldsymbol{x} - \boldsymbol{x}_A \|_2 \le R_A + \delta \}. \end{aligned} \quad (3)$$

It is well-known [17] that in obstacle-free cases, starting from the state X_{ij}, E_j can reach any point in $\mathbb{A}$ no later than P_i, while P_i can reach any point in $\mathbb{R}^2 \setminus \mathbb{A}$ before E_j. Recently, by expanding $\mathbb{A}$ to the larger region $\mathbb{A}_\delta$, the work [9] proposed the following pursuit strategy such that P_i guarantees to capture E_j in $\mathbb{A}_\delta$ and in a finite time, regardless of E_j's strategy.

Lemma 1 (Pursuit strategy, [9]). *In the absence of obstacles, from time t, if P_i adopts the pursuit strategy $\boldsymbol{u}_{P_i}(\tau) = \frac{\boldsymbol{z}(\tau)}{\|\boldsymbol{z}(\tau)\|_2}$ for all $\tau \ge t$, where $\boldsymbol{z}(\tau)$ is given by*

$$\alpha_{ij}(R_A(t) + \delta - R_A(\tau)) \frac{\boldsymbol{x}_{E_j}(\tau) - \boldsymbol{x}_{P_i}(\tau)}{\| \boldsymbol{x}_{E_j}(\tau) - \boldsymbol{x}_{P_i}(\tau) \|_2} + \boldsymbol{x}_A(\tau) - \boldsymbol{x}_A(t)$$

then regardless of E_j's strategy, P_i can ensure

(i) $\mathbb{A}(\tau) \subset \mathbb{A}_\delta(t)$ for all $\tau \ge t$;

(ii) E_j is captured in $\mathbb{A}_\delta(t)$ under $r_i = 0$ in a finite time.

We provide motivations for adopting the union set $\mathbb{A}_\delta$ of the expanded Apollonius circle and its interior, and some intuition on how it works.

Remark 1. *It is known [17], [38] that the set of points that P_i and E_j can reach along their minimum distances with a time difference $r_i/v_{P_i} \ge 0$ is a Cartesian oval, which degenerates into an Apollonius circle for $r_i = 0$. We employ the expanded Apollonius circle instead of the Cartesian oval in the pursuit strategy for both $r_i = 0$ and $r_i > 0$, for two reasons: 1) it is unclear whether a similar result to Lemma 1 still holds for a pursuit strategy based on the Cartesian oval with $r_i > 0$; 2) if P_i can guarantee to capture E_j under $r_i = 0$, then P_i can also ensure the capture under $r_i > 0$. The extension of the strategy in Lemma 1 to the Cartesian oval is not straightforward, and we leave it for future work.*

Remark 2. *Since P_i has no access to the current control input of E_j, P_i and E_j may move towards different points at the boundary of $\mathbb{A}$ at the state X_{ij}. Thus, P_i cannot guarantee to capture E_j in $\mathbb{A}$, provided that $r_i = 0$. However, introducing $\mathbb{A}_\delta$ which strictly expands $\mathbb{A}$, can generate a pursuit strategy for P_i that ensures the capture in $\mathbb{A}_\delta$. The general idea behind this strategy is that instead of focusing on points in $\mathbb{A}$, P_i can think a bit further (i.e., measured by δ) and consider the points that P_i can reach strictly before E_j. For the interested readers, please refer to [9] which proposed this strategy, for details.*

B. Onsite pursuit winning regions and strategies

We extend the results in Lemma 1 to the case of a pursuit coalition P_c against an evader E_j in the presence of obstacles.

For a pursuer P_i ($i \in c$) against E_j, we construct a region as follows. For a state X_{ij}, let $\boldsymbol{x}_{T_1}$ and $\boldsymbol{x}_{T_2}$ be two distinct points in $\mathbb{A}_\delta$ such that the line segments $\overline{\boldsymbol{x}_{P_i} \boldsymbol{x}_{T_1}}$ and $\overline{\boldsymbol{x}_{P_i} \boldsymbol{x}_{T_2}}$ are tangent to the circle $\mathbb{A}_\delta$, see Fig. 2(a). By (3), we have

$$\| \boldsymbol{x}_{T_k} - \boldsymbol{x}_A \|_2 = R_A + \delta, \ (\boldsymbol{x}_{T_k} - \boldsymbol{x}_{P_i})^\top (\boldsymbol{x}_{T_k} - \boldsymbol{x}_A) = 0$$

for $k = 1, 2$, from which we obtain

$$\begin{aligned} \boldsymbol{x}_{T_1} &= \boldsymbol{x}_A + \frac{\ell_1(\boldsymbol{x}_{P_i} - \boldsymbol{x}_A) + \ell_2(\boldsymbol{x}_{P_i} - \boldsymbol{x}_A)^\circ}{\| \boldsymbol{x}_{P_i} - \boldsymbol{x}_A \|_2^2}, \\ \boldsymbol{x}_{T_2} &= \boldsymbol{x}_A + \frac{\ell_1(\boldsymbol{x}_{P_i} - \boldsymbol{x}_A) - \ell_2(\boldsymbol{x}_{P_i} - \boldsymbol{x}_A)^\circ}{\| \boldsymbol{x}_{P_i} - \boldsymbol{x}_A \|_2^2}, \end{aligned}$$
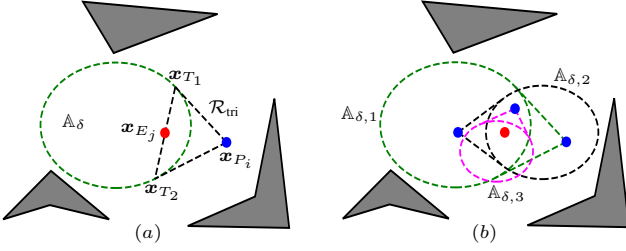
Fig. 2. Onsite pursuit winning. (a) one pursuer: if two regions $\mathbb{A}_\delta$ and $\mathcal{R}_{\text{tri}}$ surrounded by the green expanded Apollonius circle and black triangle, respectively, are obstacle-free, then P_i guarantees to capture E_j in $\mathbb{A}_\delta$ in a finite time. (b) pursuit coalition: if every pursuer in a coalition can capture an evader individually, then the evader will be captured in the intersection of all regions bounded by expanded Apollonius circles, i.e., $\cap_{i=1}^3 \mathbb{A}_{\delta,i}$.

where for a vector $\boldsymbol{x} = [x,y]^\top \in \mathbb{R}^2$, let $\boldsymbol{x}^\circ = [y,-x]^\top$, and

$$\ell_1 = (R_A + \delta)^2, \ \ell_2 = (R_A + \delta)\sqrt{\|\boldsymbol{x}_{P_i} - \boldsymbol{x}_A\|_2^2 - \ell_1}.$$

Then, we construct a region induced by X_{ij} as follows:

$$\mathcal{R}_{ij}^{\text{onsite}} = \mathcal{R}_{\text{tri}}(\boldsymbol{x}_{P_i}, \boldsymbol{x}_{T_1}, \boldsymbol{x}_{T_2}) \cup \mathbb{A}_\delta, \qquad (4)$$

which is the union of two regions with black and green boundaries in Fig. 2(a). We use $\mathcal{R}_{ij}^{\text{onsite}}$ to construct the following pursuit winning region for P_i against E_j.

Theorem 1 (Onsite pursuit winning). *At time t, if the positions X_{ij} of P_i and E_j satisfy*

$$\mathcal{R}_{ij}^{\text{onsite}}(t) \cap O = \emptyset \text{ for all } O \in \mathcal{O} \text{ and } \mathbb{A}_\delta(t) \cap \Omega_{\text{goal}} = \emptyset \ (5)$$

then using the pursuit strategy in Lemma 1 for all $\tau \geq t$, P_i can guarantee to capture E_j in $\mathbb{A}_\delta(t)$ despite E_j's strategy.

Proof. We first consider the case when there is no obstacle. If P_i adopts the pursuit strategy in Lemma 1, then starting from X_{ij} at time t, P_i can guarantee to capture E_j in $\mathbb{A}_\delta(t)$ under the point capture $r_i = 0$ and in a finite time. This also applies to our case $r_i \geq 0$ due to a larger capture range. When the obstacles are present, the same conclusion follows if we can prove that P_i using this pursuit strategy never leaves the region $\mathcal{R}_{ij}^{\text{onsite}}(t)$ before E_j is captured despite E_j's strategy. This is because $\mathcal{R}_{ij}^{\text{onsite}}(t)$ is obstacle-free and $\mathbb{A}_\delta(t)$ does not intersect with Ω_{goal} by (5).

Let $t_{\text{capture}} > t$ be the first time when E_j is captured by P_i if there is no obstacle. Next, we prove that $\boldsymbol{x}_{P_i}(\tau) \in \mathcal{R}_{ij}^{\text{onsite}}(t)$ for all $t \leq \tau \leq t_{\text{capture}}$. By Lemma 1(i), we have $\mathbb{A}(\tau) \subset \mathbb{A}_\delta(t)$ and thus by (4), $\mathbb{A}(\tau) \subset \mathcal{R}_{ij}^{\text{onsite}}(t)$. Under the pursuit strategy in Lemma 1, P_i always moves along the direction $\boldsymbol{z}(\tau)$. Then the conclusion follows if we can show that for any $t \leq \tau \leq t_{\text{capture}}$, $\boldsymbol{z}(\tau)$ consistently points from $\boldsymbol{x}_{P_i}(\tau)$ to $\mathbb{A}(\tau)$. That is, the straight line emanating from $\boldsymbol{x}_{P_i}(\tau)$ along the direction $\boldsymbol{z}(\tau)$ intersects with $\mathbb{A}(\tau)$.

Since $\boldsymbol{x}_A(\tau) - \boldsymbol{x}_{P_i}(\tau) = \alpha_{ij}^2(\boldsymbol{x}_{E_j}(\tau) - \boldsymbol{x}_{P_i}(\tau))/(\alpha_{ij}^2 - 1)$ using (2), then $\boldsymbol{z}(\tau)$ has the equivalent form

$$\alpha_{ij}(R_A(t)+\delta - R_A(\tau))\frac{\boldsymbol{x}_A(\tau) - \boldsymbol{x}_{P_i}(\tau)}{\|\boldsymbol{x}_A(\tau) - \boldsymbol{x}_{P_i}(\tau)\|_2} + \boldsymbol{x}_A(\tau) - \boldsymbol{x}_A(t).$$

Without changing $\boldsymbol{u}_{P_i}(\tau)$, by rearranging, the direction $\boldsymbol{z}(\tau)$ can be further rewritten as follows:

$$\boldsymbol{x}_A(\tau) - \boldsymbol{x}_{P_i}(\tau) + \frac{\|\boldsymbol{x}_A(\tau) - \boldsymbol{x}_{P_i}(\tau)\|_2(\boldsymbol{x}_A(\tau) - \boldsymbol{x}_A(t))}{\alpha_{ij}(R_A(t) + \delta - R_A(\tau))}$$

$$:= \boldsymbol{x}_{P_i}^\star(\tau) - \boldsymbol{x}_{P_i}(\tau),$$

where $\boldsymbol{x}_{P_i}^\star(\tau)$ is the sum of the first and third terms. Therefore, $\boldsymbol{u}_{P_i}(\tau)$ can be represented as

$$\boldsymbol{u}_{P_i}(\tau) = \frac{\boldsymbol{x}_{P_i}^\star(\tau) - \boldsymbol{x}_{P_i}(\tau)}{\|\boldsymbol{x}_{P_i}^\star(\tau) - \boldsymbol{x}_{P_i}(\tau)\|_2}, \qquad (6)$$

that is, P_i always moves towards the point $\boldsymbol{x}_{P_i}^\star(\tau)$. Since two disks $\mathbb{A}(\tau)$ and $\mathbb{A}_\delta(t)$ satisfy $\mathbb{A}(\tau) \subset \mathbb{A}_\delta(t)$, then

$$\|\boldsymbol{x}_A(\tau) - \boldsymbol{x}_A(t)\|_2 \leq R_A(t) + \delta - R_A(\tau).$$

Therefore, we have

$$\begin{aligned} \|\boldsymbol{x}_{P_i}^\star(\tau) - \boldsymbol{x}_A(\tau)\|_2 &= \frac{\|\boldsymbol{x}_A(\tau) - \boldsymbol{x}_{P_i}(\tau)\|_2 \|\boldsymbol{x}_A(\tau) - \boldsymbol{x}_A(t)\|_2}{\alpha_{ij}(R_A(t) + \delta - R_A(\tau))} \\ &\leq \frac{\|\boldsymbol{x}_A(\tau) - \boldsymbol{x}_{P_i}(\tau)\|_2}{\alpha_{ij}} \\ &= \frac{\alpha_{ij}\|\boldsymbol{x}_{P_i}(\tau) - \boldsymbol{x}_{E_j}(\tau)\|_2}{\alpha_{ij}^2 - 1} = R_A(\tau), \end{aligned}$$

where (2) is used in the last two equalities. Thus, $\boldsymbol{x}_{P_i}^\star(\tau) \in \mathbb{A}(\tau)$, implying that P_i always moves towards a point in $\mathbb{A}(\tau)$, i.e., $\boldsymbol{x}_{P_i}^\star(\tau)$. Since $\boldsymbol{x}_{P_i}(t) \in \mathcal{R}_{ij}^{\text{onsite}}(t)$ and $\mathbb{A}(\tau) \subset \mathcal{R}_{ij}^{\text{onsite}}(t)$, we have $\boldsymbol{x}_{P_i}(\tau) \in \mathcal{R}_{ij}^{\text{onsite}}(t)$ for all $t \leq \tau \leq t_{\text{capture}}$. Since (5) says there is no obstacle in $\mathcal{R}_{ij}^{\text{onsite}}(t)$, then P_i can capture E_j without hitting any obstacle. $\qquad \square$

Using Theorem 1, we then have the following onsite pursuit winning region and strategy for P_c against E_j.

Lemma 2 (Onsite pursuit winning for coalitions). *At time t, if the positions X_{cj} of P_c and E_j are such that (5) holds for all $i \in c$, then using the pursuit strategy in Lemma 1 for each pursuer P_i in P_c and all $\tau \geq t$, P_c can guarantee to capture E_j in $\cap_{i \in c}\mathbb{A}_{\delta,i}(t)$, where $\mathbb{A}_{\delta,i}(t)$ is the expanded Apollonius circle and its interior for P_i against E_j at time t.*

Proof. For each pursuer P_i ($i \in c$), since (5) holds, then by Theorem 1, P_i can capture E_j in $\mathbb{A}_{\delta,i}(t)$ on its own. Thus, this further implies that P_c can capture E_j in $\cap_{i \in c}\mathbb{A}_{\delta,i}(t)$. $\quad \square$

Remark 3. *By Lemma 2, if more pursuers satisfy (5) against one evader, then the evader is guaranteed to be captured in a smaller or equal region and in a shorter or equal time. For instance, in Fig. 2(b), three pursuers guarantee to capture the evader in the intersection of the regions bounded by three expanded Apollonius circles. Since (5) and the pursuit strategy in Lemma 1 are both independent of the other pursuers, the resulting cooperative pursuit strategy inherently allows for the distributed implementation.*

IV. CLOSE-TO-GOAL PURSUIT WINNING I: GOAL-VISIBLE CASE

For the case when the condition (5) required by the onsite pursuit winning does not hold, we propose another two pursuit winning regions and strategies for the subgames. This section

presents the first case where the pursuers can visually see the whole goal region.

A. Goal-visible points and convex goal-covering polygons

In order to construct the pursuit winning regions and strategies, we introduce several new geometric concepts and propose methods to verify or construct them. Utilising these concepts, we classify the points in Ω_{free} into two categories. Then, we investigate the pursuit winning regions and strategies when the pursuers are in each category separately, in the current and the next sections, respectively. Recall that $\Omega_{\text{free}} = \Omega_{\text{play}} \cup \Omega_{\text{goal}}$. The classification is as follows.

Definition 3 (Goal-visible point). *A point $\boldsymbol{x} \in \Omega_{\text{free}}$ is called* goal-visible *if for any point $\boldsymbol{y} \in \Omega_{\text{goal}}$, $\boldsymbol{y}$ is visible to $\boldsymbol{x}$, i.e., the line segment $\overline{\boldsymbol{xy}}$ does not intersect with obstacles in $\mathcal{O}$.*

Definition 3 shows that if a pursuer is at a goal-visible point (i.e., $\boldsymbol{x}$ in Fig. 3(a)), then it can reach any point in Ω_{goal} via an obstacle-free line segment. However, a pursuer at a non-goal-visible point (i.e., $\boldsymbol{x}$ in Fig. 3(b)) needs to change its direction in order to reach some point in Ω_{goal}. If a goal-visible point is in Ω_{play}, we next define a pair of critical points for verifying the goal-visible property and computing the pursuit strategies.
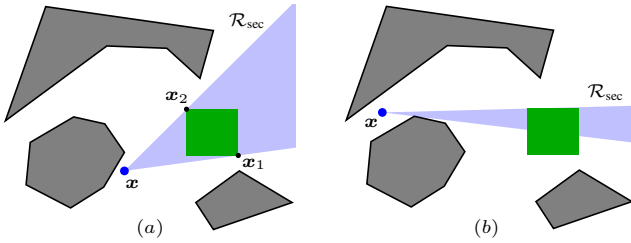

Fig. 3. (a) goal-visible point $\boldsymbol{x}$ with a pair $(\boldsymbol{x}_1, \boldsymbol{x}_2)$ of minimum-covering points: all points in Ω_{goal} are visible to $\boldsymbol{x}$ and $\Omega_{\text{goal}} \subset \mathcal{R}_{\text{sec}}(\boldsymbol{x}, \boldsymbol{x}_1, \boldsymbol{x}_2)$. (b) non-goal-visible point $\boldsymbol{x}$: at least one point in Ω_{goal} is not visible to $\boldsymbol{x}$.

Definition 4 (Pair of minimum-covering points). *For a goal-visible point $\boldsymbol{x}$ in Ω_{play}, $(\boldsymbol{x}_1, \boldsymbol{x}_2) \in \Omega_{\text{goal}}^2$ is called a* pair of minimum-covering points *for $\boldsymbol{x}$ if $\Omega_{\text{goal}} \subset \mathcal{R}_{\text{sec}}(\boldsymbol{x}, \boldsymbol{x}_1, \boldsymbol{x}_2)$.*

Let V_{goal} be the set of vertices of Ω_{goal}. As Ω_{goal} is a convex polygon, a pair of minimum-covering points for a goal-visible point $\boldsymbol{x}$ in Ω_{play} can be computed by verifying the condition $\Omega_{\text{goal}} \subset \mathcal{R}_{\text{sec}}(\boldsymbol{x}, \boldsymbol{x}_1, \boldsymbol{x}_2)$ for any two vertices $\boldsymbol{x}_1, \boldsymbol{x}_2 \in V_{\text{goal}}$. For instance, the blue region in Fig. 3(a) is the circular sector $\mathcal{R}_{\text{sec}}(\boldsymbol{x}, \boldsymbol{x}_1, \boldsymbol{x}_2)$ that covers Ω_{goal}.

Now we are ready to show the verification approach.

Lemma 3 (Verifying a goal-visible point). *A point $\boldsymbol{x} \in \Omega_{\text{free}}$ is goal-visible if and only if one of the two conditions holds: i) $\boldsymbol{x} \in \Omega_{\text{goal}}$; ii) $\boldsymbol{x} \in \Omega_{\text{play}}$ and $\mathcal{R}_{\text{tri}}(\boldsymbol{x}, \boldsymbol{x}_1, \boldsymbol{x}_2) \cap O = \emptyset$ for all $O \in \mathcal{O}$, where $(\boldsymbol{x}_1, \boldsymbol{x}_2) \in \Omega_{\text{goal}}^2$ is a pair of minimum-covering points for $\boldsymbol{x}$.*

Proof. Regarding i), all points in Ω_{goal} are goal-visible by Definition 3, as Ω_{goal} is obstacle-free and convex.

Regarding ii), if $\boldsymbol{x} \in \Omega_{\text{play}}$ and $\mathcal{R}_{\text{tri}}(\boldsymbol{x}, \boldsymbol{x}_1, \boldsymbol{x}_2) \cap O = \emptyset$ for all $O \in \mathcal{O}$, then by Definition 4 and the convexity of Ω_{goal}, the line segment $\overline{\boldsymbol{xy}}$ does not intersect with the obstacles for all

$\boldsymbol{y} \in \Omega_{\text{goal}}$, i.e., $\boldsymbol{x}$ is goal-visible, where $\boldsymbol{x}_1, \boldsymbol{x}_2 \in \mathbb{R}^2$ are a pair of minimum-covering points for $\boldsymbol{x}$. Conversely, if $\boldsymbol{x} \in \Omega_{\text{play}}$ is goal-visible, then by Definition 3, the line segment $\overline{\boldsymbol{xy}}$ does not intersect with the obstacles for all $\boldsymbol{y} \in \Omega_{\text{goal}}$ and thus for all $\boldsymbol{y}$ at the line segment $\overline{\boldsymbol{x}_1 \boldsymbol{x}_2}$. Therefore, $\mathcal{R}_{\text{tri}}(\boldsymbol{x}, \boldsymbol{x}_1, \boldsymbol{x}_2) \cap O = \emptyset$ for all $O \in \mathcal{O}$, which completes the proof. $\square$

We construct a class of polygons, which can ensure the consistent goal-visible property and will be used in synthesizing pursuit winning strategies below.

Definition 5 (Convex goal-covering polygon). *A polygon $\mathcal{R} \subset \mathbb{R}^2$ is a* convex goal-covering polygon (GCP) *for a goal-visible point $\boldsymbol{x} \in \Omega_{\text{free}}$ if i) $\mathcal{R}$ is convex, ii) $\boldsymbol{x} \in \mathcal{R}$, iii) $\mathcal{R} \subset \Omega_{\text{free}}$ and iv) Ω_{goal} is covered by $\mathcal{R}$ (i.e., $\Omega_{\text{goal}} \subset \mathcal{R}$).*

As an illustration, the orange regions in Fig. 4 are convex GCPs for the underlying points $\boldsymbol{x}$, differing in whether $\boldsymbol{x}$ is at the boundary of the convex GCP. The following lemma shows that such convex GCPs always exist and possess the following consistent property.
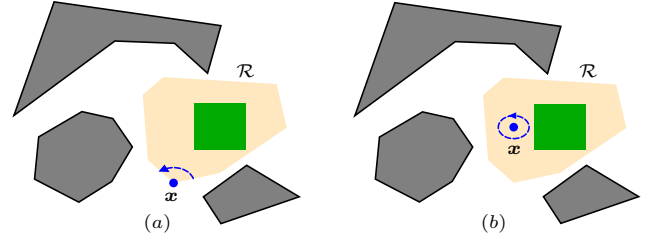

Fig. 4. Convex goal-covering polygon (GCP). The orange polygon $\mathcal{R}$ is a convex GCP for $\boldsymbol{x}$, as i) $\mathcal{R}$ is convex, ii) $\boldsymbol{x} \in \mathcal{R}$, iii) $\mathcal{R} \subset \Omega_{\text{free}}$ and $\Omega_{\text{goal}} \subset \mathcal{R}$. (a) if $\boldsymbol{x}$ is at the boundary of $\mathcal{R}$, the direction range $D_{\mathcal{R}}(\boldsymbol{x})$ is the blue direction range; otherwise (b) $D_{\mathcal{R}}(\boldsymbol{x}) = [0, 2\pi)$.

Lemma 4 (Existence and consistency). *If a point $\boldsymbol{x} \in \Omega_{\text{free}}$ is goal-visible, then there must exist a convex GCP for $\boldsymbol{x}$. If $\mathcal{R} \subset \Omega_{\text{free}}$ is a convex GCP for some goal-visible point, then all points in $\mathcal{R}$ are goal-visible.*

Proof. Regarding the existence, consider a goal-visible point $\boldsymbol{x} \in \Omega_{\text{free}}$. If $\boldsymbol{x} \in \Omega_{\text{goal}}$, then Ω_{goal} is a natural convex GCP for $\boldsymbol{x}$. If $\boldsymbol{x} \in \Omega_{\text{play}}$, then by Definition 4 there exist a pair of minimum-covering points $(\boldsymbol{x}_1, \boldsymbol{x}_2) \in \Omega_{\text{goal}}^2$ for $\boldsymbol{x}$, where $\boldsymbol{x}_1$ and $\boldsymbol{x}_2$ are two vertices of Ω_{goal}, i.e., $\boldsymbol{x}_1, \boldsymbol{x}_2 \in V_{\text{goal}}$. Let S be the set of vertices in V_{goal} which are not in $\mathcal{R}_{\text{tri}}(\boldsymbol{x}, \boldsymbol{x}_1, \boldsymbol{x}_2)$. Since Ω_{goal} is a convex polygon and $\Omega_{\text{goal}} \subset \mathcal{R}_{\text{sec}}(\boldsymbol{x}, \boldsymbol{x}_1, \boldsymbol{x}_2)$, then the vertex set $S \cup \{\boldsymbol{x}, \boldsymbol{x}_1, \boldsymbol{x}_2\}$ forms a convex polygon $\mathcal{R}$ that covers Ω_{goal}. Thus, $\mathcal{R}$ satisfies the conditions i), ii) and iv) in Definition 5. As $\boldsymbol{x}$ is goal-visible, then $\mathcal{R}_{\text{tri}}(\boldsymbol{x}, \boldsymbol{x}_1, \boldsymbol{x}_2)$ is obstacle-free. Recall that $\Omega_{\text{goal}} \subset \Omega_{\text{free}}$. Hence, we obtain that $\mathcal{R} \subset \Omega_{\text{free}}$ and therefore $\mathcal{R}$ is a convex GCP for $\boldsymbol{x}$.

Regarding the consistency, since $\mathcal{R}$ is convex and obstacle-free and covers Ω_{goal}, then all points in $\mathcal{R}$ have obstacle-free line segments to any point in Ω_{goal}, i.e., all points in $\mathcal{R}$ are goal-visible. $\square$

Remark 4. *Lemma 4 implies that, if a pursuer is at a goal-visible point, then moving towards any point in a convex GCP (it indeed exists) for this goal-visible point can ensure that the pursuer is goal-visible consistently.*

The following concept is proposed to characterize the set of moving directions in a convex GCP in Remark 4 that preserve the goal-visible property.

Definition 6 (Direction range in a convex GCP). *Let $\mathcal{R}$ be a convex GCP for a goal-visible point $\boldsymbol{x} \in \Omega_{\text{free}}$. The direction range of $\boldsymbol{x}$ in $\mathcal{R}$, denoted by $D_{\mathcal{R}}(\boldsymbol{x}) \subset [0, 2\pi)$, is the set of angles $\{\sigma(\boldsymbol{x}, \boldsymbol{y}) \mid \boldsymbol{y} \neq \boldsymbol{x}, \boldsymbol{y} \in \mathcal{R}\}$.*

The direction range can be easily identified as follows.

Remark 5. *Let $\mathcal{R}$ be a convex GCP for a goal-visible point $\boldsymbol{x}$. As in Fig. 4(a), if $\boldsymbol{x}$ is at the boundary of $\mathcal{R}$, then $D_{\mathcal{R}}(\boldsymbol{x}) = D[\theta^L, \theta^U]$, where $\theta^L, \theta^U \in [0, 2\pi)$ are two directions of the edges from $\boldsymbol{x}$ along $\mathcal{R}$'s boundary. As in Fig. 4(b), if $\boldsymbol{x}$ is in the interior of $\mathcal{R}$, then $D_{\mathcal{R}}(\boldsymbol{x}) = [0, 2\pi)$.*

B. Goal-visible pursuit winning

We consider the first category where all pursuers in a pursuit coalition P_c are goal-visible (i.e., lie at goal-visible points). The following concept for the obstacle-free case introduced in [17] is required for the strategy synthesis below.

Definition 7 (Evasion region). *Given a state X_{cj}, the evasion region is the set of points in $\mathbb{R}^2$ that E_j can reach prior to the capture by P_c, regardless of P_c's strategy, in the absence of obstacles.*

According to [40], the closure of the evasion region, denoted by $\mathbb{E}(c, j)$, is bounded, strictly convex and given by

$$\mathbb{E}(c, j) = \{\boldsymbol{x} \in \mathbb{R}^2 \mid f_{ij}(\boldsymbol{x}, X_{ij}) \geq 0, i \in c\}, \quad (7)$$

where $f_{ij} : \mathbb{R}^2 \times \mathbb{R}^2 \times \mathbb{R}^2 \to \mathbb{R}$ for $i \in c$ is defined as

$$f_{ij}(\boldsymbol{x}, X_{ij}) = \|\boldsymbol{x} - \boldsymbol{x}_{P_i}\|_2 - \alpha_{ij}\|\boldsymbol{x} - \boldsymbol{x}_{E_j}\|_2 - r_i.$$

Note that the Apollonius circle is a special case of the evasion region's boundary when $r_i = 0$. Then, the *safe distance* of X_{cj}, denoted by $\varrho(X_{cj})$, is defined as the signed distance between $\mathbb{E}(c, j)$ and Ω_{goal}, which can be computed using the convex optimization below.

Definition 8 (Safe distance). *For a state X_{cj}, let $(\boldsymbol{x}_I, \boldsymbol{x}_G)$ be the solution of the convex optimization problem $\mathcal{P}(X_{cj})$:*

$$\begin{aligned} \underset{(\boldsymbol{x}, \boldsymbol{y}) \in \mathbb{R}^2 \times \mathbb{R}^2}{\text{minimize}} \quad & \|\boldsymbol{x} - \boldsymbol{y}\|_2 \\ \text{subject to} \quad & f_{ij}(\boldsymbol{x}, X_{ij}) \geq 0, \, \forall i \in c \\ & A_m \boldsymbol{y} + \boldsymbol{b}_m \geq 0, \, \forall m \in I_{\text{goal}}. \end{aligned} \quad (8)$$

If 1) $\boldsymbol{x}_I = \boldsymbol{x}_G$ and $f_{ij}(\boldsymbol{x}_I, X_{ij}) > 0$ for all $i \in c$, or 2) $\boldsymbol{x}_I = \boldsymbol{x}_G$ and $A_m \boldsymbol{x}_I + \boldsymbol{b}_m > 0$ for all $m \in I_{\text{goal}}$, then $\varrho(X_{cj}) = -\infty$, and $\varrho(X_{cj}) = \|\boldsymbol{x}_I - \boldsymbol{x}_G\|_2$ otherwise.

In order to construct the pursuit winning region and strategy, we next present a sufficient condition on the pursuit strategies to ensure the goal-visible consistency.

Lemma 5 (Consistent goal-visible pursuit strategy). *At time t, suppose that $\boldsymbol{x}_{P_i}$ is goal-visible. If a pursuit strategy $\boldsymbol{u}_{P_i}(\tau) = [\cos\theta_i(\tau), \sin\theta_i(\tau)]^\top$ is such that P_i moves towards a point in a convex GCP $\mathcal{R}_i(\tau)$ for $\boldsymbol{x}_{P_i}(\tau)$, i.e., $\theta_i(\tau) \in D_{\mathcal{R}_i(\tau)}(\boldsymbol{x}_{P_i}(\tau))$ for all $\tau \geq t$, then $\boldsymbol{x}_{P_i}(\tau)$ is goal-visible for all $\tau \geq t$.*
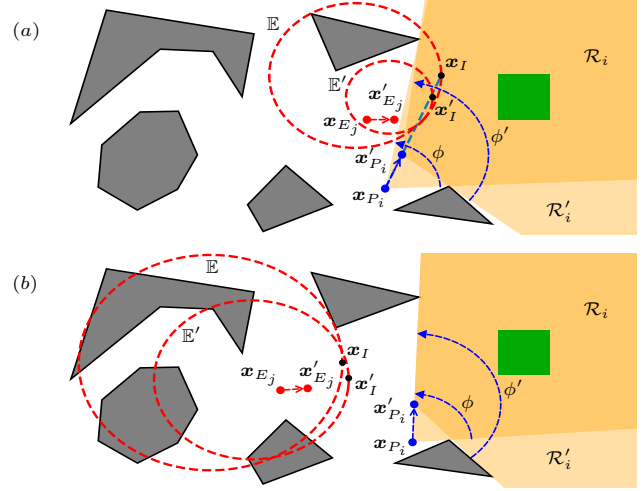

Fig. 5. Goal-visible pursuit winning. If P_i is goal-visible and the safe distance (i.e., the distance between the region $\mathbb{E}$ (red boundary) and Ω_{goal}) is non-negative, then P_i guarantees to win against E_j, which also applies to a pursuit coalition. Let $\mathcal{R}_i$ be a (orange) convex GCP for $\boldsymbol{x}_{P_i}$ with the direction angle span ϕ. The pursuit winning strategy, which ensures the consistent goal-visible property, is as follows. (a) If the closest point $\boldsymbol{x}_I$ in $\mathbb{E}$ to Ω_{goal} is in the angle span ϕ, then P_i moves towards $\boldsymbol{x}_I$. (b) If $\boldsymbol{x}_I$ is not in ϕ, then P_i moves along one edge of $\mathcal{R}_i$. After a small time step, P_i reaches $\boldsymbol{x}'_{P_i}$ which is goal-visible and has a convex GCP $\mathcal{R}'_i$ with the angle span ϕ'. The evader and the closest point are updated to $\boldsymbol{x}'_{E_j}$ and $\boldsymbol{x}'_I$, respectively.

Proof. Since $\boldsymbol{x}_{P_i}(t)$ is goal-visible, then according to Lemma 4 there exists a convex GCP $\mathcal{R}_i(t)$ for $\boldsymbol{x}_{P_i}(t)$. Since $\boldsymbol{x}_{P_i}(t) \in \mathcal{R}_i(t)$ by Definition 5 and P_i moves towards a point in $\mathcal{R}_i(t)$ under the input $\boldsymbol{u}_{P_i}(t)$ (i.e., $\theta_i(t) \in D_{\mathcal{R}_i(t)}(\boldsymbol{x}_{P_i}(t))$), then after moving along $\boldsymbol{u}_{P_i}(t)$ with a small time interval $\Delta t > 0$, we have $\boldsymbol{x}_{P_i}(t + \Delta t) \in \mathcal{R}_i(t)$ (note that $\mathcal{R}_i(t)$ is convex). Then, the consistency in Lemma 4 shows that $\boldsymbol{x}_{P_i}(t + \Delta t)$ is goal-visible for which there exists a convex GCP $\mathcal{R}_i(t + \Delta t)$. Thus, the conclusion follows by the similar argument for $\boldsymbol{x}_{P_i}(t + \Delta t)$ and the increasing iteration. $\square$

Utilising the safe distance, goal visibility and convex GCPs, we next present the pursuit winning region and strategy for the goal-visible case of the close-to-goal pursuit winning, as illustrated in Fig. 5.

Theorem 2 (Goal-visible pursuit winning). *At time t, if the positions X_{cj} of P_c and E_j are such that*

1) $\boldsymbol{x}_{P_i}$ is goal-visible for all $i \in c$;
2) the safe distance is non-negative, i.e., $\varrho(X_{cj}) \geq 0$;

then $\boldsymbol{x}_{P_i}(\tau)$ is goal-visible for all $\tau \geq t$ and all $i \in c$, and P_c can guarantee to win against E_j, regardless of E_j's strategy, by using the pursuit strategy for all $i \in c$ as follows:

$$\boldsymbol{u}_{P_i}(\tau) = [\cos\theta_i(\tau), \sin\theta_i(\tau)]^\top \quad (9)$$

for all $\tau \geq t$, where

$$\theta_i(\tau) = \text{argmin}_{\theta \in D_{\mathcal{R}_i(\tau)}(\boldsymbol{x}_{P_i}(\tau))} |\theta - \sigma(\boldsymbol{x}_{P_i}(\tau), \boldsymbol{x}_I(\tau))| \quad (10)$$

In (10), $D_{\mathcal{R}_i(\tau)}(\boldsymbol{x}_{P_i}(\tau))$ is the direction range of $\boldsymbol{x}_{P_i}(\tau)$ in a convex GCP $\mathcal{R}_i(\tau)$ and $(\boldsymbol{x}_I(\tau), \boldsymbol{x}_G(\tau))$ is the optimal solution to $\mathcal{P}(X_{cj}(\tau))$ in (8).

Proof. The conclusion follows if we can prove that under the pursuit strategy (9), $\boldsymbol{x}_{P_i}(\tau)$ is goal-visible for all $i \in c$ and the safe distance is non-negative, i.e., $\varrho(X_{cj}(\tau)) \geq 0$ (note that $\boldsymbol{x}_{E_j}(\tau) \in \mathbb{E}(c,j)$ before E_j is captured), for all $\tau \geq t$. This holds for $\tau = t$ due to the conditions 1) and 2).

We first prove the consistent goal-visible property under the strategy (9). Note that $\boldsymbol{x}_{P_i}(t)$ is goal-visible and (9) indicates that $\theta_i(\tau) \in D_{\mathcal{R}_i(\tau)}(\boldsymbol{x}_{P_i}(\tau))$ for all $\tau \geq t$. Then, by Lemma 5 we obtain that $\boldsymbol{x}_{P_i}(\tau)$ is goal-visible for all $\tau \geq t$ and $i \in c$, where a convex GCP $\mathcal{R}_i(\tau)$ exists by the proof of Lemma 5.

We show the consistent non-negative safe distance under the strategy (9), i.e., $\varrho(X_{cj}(\tau)) \geq 0$ for all $\tau \geq t$. At time τ, let $(\boldsymbol{x}_I(\tau), \boldsymbol{x}_G(\tau))$ be the optimal solution to $\mathcal{P}(X_{cj}(\tau))$ in (8) and $\theta_i^\star(\tau) = \sigma(\boldsymbol{x}_{P_i}(\tau), \boldsymbol{x}_I(\tau))$. There are two possible cases.

Case 1: $\theta_i^\star(\tau) \in D_{\mathcal{R}_i(\tau)}(\boldsymbol{x}_{P_i}(\tau))$ for all $i \in c$, where one pursuer case is shown in Fig. 5(a) and ϕ is the angle span of $D_{\mathcal{R}_i(\tau)}(\boldsymbol{x}_{P_i}(\tau))$. Then, (10) implies that $\theta_i(\tau) = \theta_i^\star(\tau)$ and thus the strategy (9) becomes

$$\boldsymbol{u}_{P_i}(\tau) = [\cos\theta_i^\star(\tau), \sin\theta_i^\star(\tau)]^\top = \frac{\boldsymbol{x}_I(\tau) - \boldsymbol{x}_{P_i}(\tau)}{\|\boldsymbol{x}_I(\tau) - \boldsymbol{x}_{P_i}(\tau)\|_2}. \tag{11}$$

If $\varrho(X_{cj}(\tau)) \geq 0$, then $(\boldsymbol{x}_I(\tau), \boldsymbol{x}_G(\tau))$ is the unique optimal solution to $\mathcal{P}(X_{cj}(\tau))$ in (8), as $\mathbb{E}(c,j)$ is strictly convex and Ω_{goal} is convex. For notation simplicity, we let $d(\boldsymbol{x}, \boldsymbol{y}) = \|\boldsymbol{x} - \boldsymbol{y}\|_2$ for $\boldsymbol{x}, \boldsymbol{y} \in \mathbb{R}^2$, and omit the time argument τ temporarily here. According to the *Karush-Kuhn-Tucker (KKT) conditions*, the solution $(\boldsymbol{x}_I, \boldsymbol{x}_G)$ satisfies

$$\boldsymbol{0} = \nabla_{\boldsymbol{x}} d(\boldsymbol{x}_I, \boldsymbol{x}_G) + \sum\nolimits_{i \in c} \lambda_i \nabla_{\boldsymbol{x}} f_{ij}(\boldsymbol{x}_I, X_{ij})$$
$$\boldsymbol{0} = \nabla_{\boldsymbol{y}} d(\boldsymbol{x}_I, \boldsymbol{x}_G) + \sum\nolimits_{m \in I_{\text{goal}}} \lambda_m A_m$$
$$f_{ij}(\boldsymbol{x}_I, X_{ij}) \geq 0, \ \lambda_i \leq 0, \ \lambda_i f_{ij}(\boldsymbol{x}_I, X_{ij}) = 0, \ i \in c$$
$$A_m \boldsymbol{x}_G + \boldsymbol{b}_m \geq 0, \lambda_m \leq 0, \lambda_m(A_m \boldsymbol{x}_G + \boldsymbol{b}_m) = 0, m \in I_{\text{goal}} \tag{12}$$

where $\lambda_i, \lambda_m \in \mathbb{R}$ are the Lagrange multipliers, and $\nabla_{\boldsymbol{x}}$ and $\nabla_{\boldsymbol{y}}$ represent the gradient operators with respect to $\boldsymbol{x}$ and $\boldsymbol{y}$, respectively. The slackness condition on $\boldsymbol{x}_G$ in (12) implies that the index set I_{goal} can be classified into two disjoint index sets $I_{\text{goal}}^{=0}$ and $I_{\text{goal}}^{>0}$ where

$$\begin{cases} A_m \boldsymbol{x}_G + \boldsymbol{b}_m = 0, \ \lambda_m \leq 0, & \text{if } m \in I_{\text{goal}}^{=0} \\ A_m \boldsymbol{x}_G + \boldsymbol{b}_m > 0, \ \lambda_m = 0, & \text{if } m \in I_{\text{goal}}^{>0}. \end{cases} \tag{13}$$

Then, the speed of the closure $\mathbb{E}(c,j)$ of the evasion region moving away from Ω_{goal}, i.e., $\dot{\varrho}(X_{cj})$, can be computed as

$$\begin{aligned} \dot{\varrho}(X_{cj}) &= \frac{d}{dt} d(\boldsymbol{x}_I, \boldsymbol{x}_G) \\ &= \nabla_{\boldsymbol{x}}^\top d(\boldsymbol{x}_I, \boldsymbol{x}_G) \dot{\boldsymbol{x}}_I + \nabla_{\boldsymbol{y}}^\top d(\boldsymbol{x}_I, \boldsymbol{x}_G) \dot{\boldsymbol{x}}_G \\ &= -\sum\nolimits_{i \in c} \lambda_i \nabla_{\boldsymbol{x}}^\top f_{ij}(\boldsymbol{x}_I, X_{ij}) \dot{\boldsymbol{x}}_I - \sum\nolimits_{m \in I_{\text{goal}}} \lambda_m A_m^\top \dot{\boldsymbol{x}}_G \\ &= -\sum\nolimits_{i \in c} \lambda_i \nabla_{\boldsymbol{x}}^\top f_{ij}(\boldsymbol{x}_I, X_{ij}) \dot{\boldsymbol{x}}_I - \sum\nolimits_{m \in I_{\text{goal}}^{=0}} \lambda_m A_m^\top \dot{\boldsymbol{x}}_G \\ &= -\sum\nolimits_{i \in c} \lambda_i \nabla_{\boldsymbol{x}}^\top f_{ij}(\boldsymbol{x}_I, X_{ij}) \dot{\boldsymbol{x}}_I \end{aligned}$$

where the third and forth equalities follow from (12) and (13), respectively. The last equality follows due to the fact that for $m \in I_{\text{goal}}^{=0}$, $\boldsymbol{x}_G$ is always at the boundary $A_m \boldsymbol{x}_G + \boldsymbol{b}_m = 0$, and thus $A_m^\top \dot{\boldsymbol{x}}_G = 0$. Then, by following the similar argument

in the proof of [40, Theorem 3.1], we can obtain that if every pursuer in P_c adopts the strategy (11), then $\dot{\varrho}(X_{cj}) \geq 0$. This guarantees that the safe distance will not strictly decrease and therefore the non-negative property holds for all $\tau \geq t$, as $\varrho(X_{cj}(\tau)) \geq 0$ initially, i.e., when $\tau = t$.

Case 2: there exist a subset $\bar{c}$ of pursuers in c such that $\theta_i^\star(\tau) \notin D_{\mathcal{R}_i(\tau)}(\boldsymbol{x}_{P_i}(\tau))$ for all $i \in \bar{c}$, where one pursuer case is in Fig. 5(b). The strategy (9) indicates that each pursuer in $\bar{c}$ moves along the direction $\theta_i(\tau)$ which is different from $\theta_i^\star(\tau)$. Thus, the safe distance may decrease, i.e., $\dot{\varrho}(X_{cj}(\tau)) < 0$, as $\mathbb{E}(c,j)$ may approach Ω_{goal}. However, since $\boldsymbol{x}_{P_i}(\tau)$ is goal-visible for all $\tau \geq t$ and $i \in c$ under (9), the direction from $\boldsymbol{x}_{P_i}(\tau)$ to any point in Ω_{goal} is in $D_{\mathcal{R}_i(\tau)}(\boldsymbol{x}_{P_i}(\tau))$. Thus, there must exist $\tau' \geq \tau$ such that $\theta_i^\star(\tau') \in D_{\mathcal{R}_i(\tau')}(\boldsymbol{x}_{P_i}(\tau'))$ for all $i \in c$ before $\mathbb{E}(c,j)$ intersects with the interior of Ω_{goal}, i.e., a negative safe distance. This implies that we go back to Case 1 for which the non-negative safe distance is guaranteed under the strategy (11). Thus, we complete the proof. $\square$

Remark 6. *Since the safe distance in Definition 8 is defined by ignoring obstacles, the proof of Lemma 3.3 in [40] where at most three pursuers are needed to ensure the winning in the three-dimensional space, can be easily adapted to prove that if a pursuit coalition is able to defend the goal region against an evader via the goal-visible pursuit winning, then at most two pursuers in the coalition are necessarily needed.*

Note that the pursuit winning strategy in Theorem 2 requires a convex GCP $\mathcal{R}_i(\tau)$ for the goal-visible point $\boldsymbol{x}_{P_i}(\tau)$ at time τ for all $i \in c$, which exists by Lemma 4. If $(\boldsymbol{x}_1, \boldsymbol{x}_2)$ is a pair of minimum-covering points for $\boldsymbol{x}_{P_i}(\tau)$, then as Fig. 3(a) indicates, there exists a convex GCP $\mathcal{R}_i(\tau)$ such that

$$D_{\mathcal{R}_i(\tau)}(\boldsymbol{x}_{P_i}(\tau)) = D[\sigma(\boldsymbol{x}_{P_i}(\tau), \boldsymbol{x}_1), \sigma(\boldsymbol{x}_{P_i}(\tau), \boldsymbol{x}_2)]. \tag{14}$$

However, if Ω_{goal} is a small region, then the direction range (14) has a small angle span and thus under the strategy (9), the pursuer will finally move closely around or in Ω_{goal}. In order to achieve a larger range of movement for the pursuers, we next present a method to construct another class of convex GCPs. Let V_{obs} be the set of the vertices of obstacles in $\mathcal{O}$. We first introduce the following specific vertices. Recall that for two angles θ_1 and θ_2, $D[\theta_1, \theta_2]$ is the set of angles from θ_1 to θ_2 in a counterclockwise direction, and $|D[\theta_1, \theta_2]|$ is the angle span of $D[\theta_1, \theta_2]$.

Definition 9 (First-visible obstacle vertex). *For a goal-visible point $\boldsymbol{x} \in \Omega_{\text{play}}$, a pair of obstacle vertices $(\boldsymbol{y}^L, \boldsymbol{y}^U) \in V_{\text{obs}}^2$ is* first-visible *for $\boldsymbol{x}$ if*

$$\begin{aligned} \boldsymbol{y}^L = \operatorname{argmin}_{\boldsymbol{y} \in V_{\text{obs}}} \quad & |D[\sigma(\boldsymbol{x}, \boldsymbol{y}), \sigma(\boldsymbol{x}, \boldsymbol{x}^L)]| \\ \text{subject to} \quad & |D[\sigma(\boldsymbol{x}, \boldsymbol{y}), \sigma(\boldsymbol{x}, \boldsymbol{x}^L)]| \leq \pi \\ & |D[\sigma(\boldsymbol{x}, \boldsymbol{y}), \sigma(\boldsymbol{x}, \boldsymbol{x}^U)]| \leq \pi \\ & \overline{\boldsymbol{x}\boldsymbol{y}} \text{ is obstacle-free} \end{aligned} \tag{15}$$

$$\begin{aligned} \boldsymbol{y}^U = \operatorname{argmin}_{\boldsymbol{y} \in V_{\text{obs}}} \quad & |D[\sigma(\boldsymbol{x}, \boldsymbol{x}^U), \sigma(\boldsymbol{x}, \boldsymbol{y})]| \\ \text{subject to} \quad & |D[\sigma(\boldsymbol{x}, \boldsymbol{x}^U), \sigma(\boldsymbol{x}, \boldsymbol{y})]| \leq \pi \\ & |D[\sigma(\boldsymbol{x}, \boldsymbol{x}^L), \sigma(\boldsymbol{x}, \boldsymbol{y})]| \leq \pi \\ & \overline{\boldsymbol{x}\boldsymbol{y}} \text{ is obstacle-free} \end{aligned} \tag{16}$$
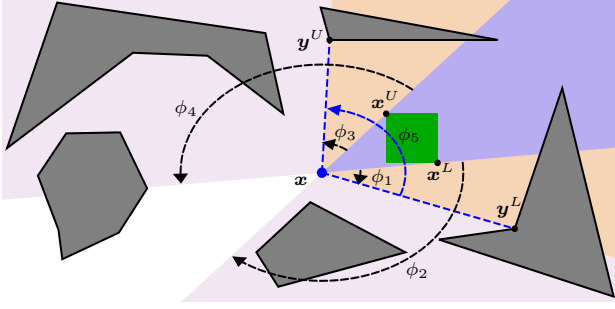
Fig. 6. First-visible obstacle vertices $\boldsymbol{y}^L$ and $\boldsymbol{y}^U$. For a goal-visible point $\boldsymbol{x}$ with a pair of minimum-covering points $(\boldsymbol{x}^L, \boldsymbol{x}^U)$, $\boldsymbol{y}^L$ is the first visible obstacle vertex when rotating $\sigma(\boldsymbol{x}, \boldsymbol{x}^L)$ in a clockwise direction (i.e., span ϕ_1) before hitting $\sigma(\boldsymbol{x}^U, \boldsymbol{x})$ (i.e., until span ϕ_2). If there is no such vertex, $\boldsymbol{y}^L = 2\boldsymbol{x} - \boldsymbol{x}^U$ is the symmetry point to $\boldsymbol{x}^U$ with respect to $\boldsymbol{x}$. The point $\boldsymbol{y}^U$ is defined similarly but in a counterclockwise direction from $\sigma(\boldsymbol{x}, \boldsymbol{x}^U)$.

where $(\boldsymbol{x}^L, \boldsymbol{x}^U)$ is a pair of minimum-covering points for $\boldsymbol{x}$. If the problem (15) *is infeasible, we define $\boldsymbol{y}^L = 2\boldsymbol{x} - \boldsymbol{x}^U$, and if the problem* (16) *is infeasible, we define $\boldsymbol{y}^U = 2\boldsymbol{x} - \boldsymbol{x}^L$.*

Remark 7. *The first-visible obstacle vertex in Definition 9 is described geometrically in Fig. 6. Recall that $(\boldsymbol{x}^L, \boldsymbol{x}^U)$ is a pair of minimum-covering points for $\boldsymbol{x}$. Then, $\boldsymbol{y}^L$ is the first visible obstacle vertex when rotating $\sigma(\boldsymbol{x}, \boldsymbol{x}^L)$ centered at $\boldsymbol{x}$ in a clockwise direction (i.e., span ϕ_1) before hitting $\sigma(\boldsymbol{x}^U, \boldsymbol{x})$ (i.e., until span ϕ_2). If there is no such vertex, $\boldsymbol{y}^L = 2\boldsymbol{x} - \boldsymbol{x}^U$ is the symmetry point to $\boldsymbol{x}^U$ with respect to $\boldsymbol{x}$. The point $\boldsymbol{y}^U$ is defined similarly but is counterclockwise from $\sigma(\boldsymbol{x}, \boldsymbol{x}^U)$.*

Using the first-visible obstacle vertices, we next construct a class of convex GCPs that achieve a larger range of movement than (14) for the pursuers, illustrated in Fig. 7 if $\boldsymbol{x}_{P_i} \in \Omega_{\text{play}}$.

Theorem 3 (Constructing convex GCPs). *For a goal-visible $\boldsymbol{x}_{P_i} \in \Omega_{\text{free}}$, if $\boldsymbol{x}_{P_i} \in \Omega_{\text{goal}}$, then there exists a convex GCP $\mathcal{R}_i$ such that $D_{\mathcal{R}_i}(\boldsymbol{x}_{P_i}) = [0, 2\pi)$; if $\boldsymbol{x}_{P_i} \in \Omega_{\text{play}}$, then there exists a convex GCP $\mathcal{R}_i$ such that $D_{\mathcal{R}_i}(\boldsymbol{x}_{P_i})$ is given by*

$$\begin{cases} D[\theta^L, \theta^U], & \text{if } |D[\theta^L, \theta^U]| \le \pi \\ D[\theta^L, \theta^L + \pi] \text{ or } D[\theta^U - \pi, \theta^U], & \text{otherwise} \end{cases} \tag{17}$$

where $\theta^L = \sigma(\boldsymbol{x}_{P_i}, \boldsymbol{y}^L)$, $\theta^U = \sigma(\boldsymbol{x}_{P_i}, \boldsymbol{y}^U)$ and $(\boldsymbol{y}^L, \boldsymbol{y}^U)$ is a pair of first-visible obstacle vertices for $\boldsymbol{x}_{P_i}$.

Proof. Consider a goal-visible point $\boldsymbol{x}_{P_i} \in \Omega_{\text{free}}$. If $\boldsymbol{x}_{P_i} \in \Omega_{\text{goal}}$, then Ω_{goal} is a natural convex GCP for $\boldsymbol{x}_{P_i}$. Note that Ω_{goal} does not intersect with the obstacles. We can expand Ω_{goal} by moving each edge of Ω_{goal} along its outward normal vector with a small distance and obtain a larger convex GCP $\mathcal{R}_i$ for $\boldsymbol{x}_{P_i}$ such that $\boldsymbol{x}_{P_i}$ is in the interior of $\mathcal{R}_i$. Therefore, by Remark 5 we have $D_{\mathcal{R}_i}(\boldsymbol{x}_{P_i}) = [0, 2\pi)$.

We next construct a convex GCP for $\boldsymbol{x}_{P_i} \in \Omega_{\text{play}}$, depicted in Fig. 7. Let $(\boldsymbol{x}^L, \boldsymbol{x}^U)$ be a pair of minimum-covering points and $(\boldsymbol{y}^L, \boldsymbol{y}^U)$ a pair of first-visible obstacle vertices for $\boldsymbol{x}_{P_i}$. Also let $\theta^L = \sigma(\boldsymbol{x}_{P_i}, \boldsymbol{y}^L)$ and $\theta^U = \sigma(\boldsymbol{x}_{P_i}, \boldsymbol{y}^U)$. There are two cases depending on whether $|D[\theta^L, \theta^U]| \le \pi$ holds, which will be discussed separately.

Case 1: $|D[\theta^L, \theta^U]| \le \pi$, shown in Fig. 7(a). We first focus on the part on θ^L. We extend the farther boundary of Ω_{goal}
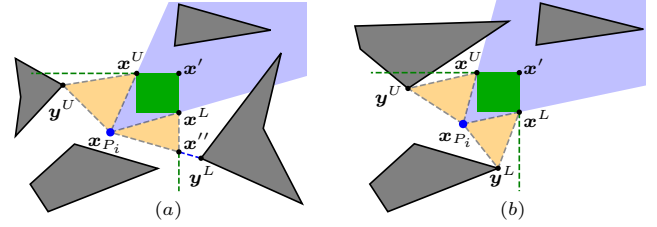

Fig. 7. Convex GCPs via first-visible obstacle vertices. Let $\theta^L = \sigma(\boldsymbol{x}_{P_i}, \boldsymbol{y}^L)$ and $\theta^U = \sigma(\boldsymbol{x}_{P_i}, \boldsymbol{y}^U)$. All orange regions are proved to be obstacle-free. (a) if $|D[\theta^L, \theta^U]| \le \pi$, then the region (counterclockwise vertices $\boldsymbol{x}_{P_i}, \boldsymbol{x}''$, $\boldsymbol{x}', \boldsymbol{x}^U, \boldsymbol{y}^U$) is a convex GCP for $\boldsymbol{x}_{P_i}$. (b) if $|D[\theta^L, \theta^U]| > \pi$, then two regions (vertices $\boldsymbol{x}_{P_i}, \boldsymbol{y}^L, \boldsymbol{x}^L, \boldsymbol{x}', \boldsymbol{x}^U$) and (vertices $\boldsymbol{x}_{P_i}, \boldsymbol{x}^L, \boldsymbol{x}', \boldsymbol{x}^U, \boldsymbol{y}^U$) can be expanded into convex GCPs for $\boldsymbol{x}_{P_i}$ such that the direction ranges for $\boldsymbol{x}_{P_i}$ are $D[\theta^L, \theta^L + \pi]$ and $D[\theta^U - \pi, \theta^U]$, respectively.

that goes through $\boldsymbol{x}^L$, and then obtain an intersection point $\boldsymbol{x}''$ with the line segment $\overline{\boldsymbol{x}_{P_i}\boldsymbol{y}^L}$ (if there is no intersection as in the case for θ^U, we take $\boldsymbol{y}^U$). For notation convenience, we define the following polygons via vertices:

$$\mathcal{R}_0 : \text{counterclockwise vertices } \boldsymbol{x}_{P_i}, \boldsymbol{x}^L, \boldsymbol{x}', \boldsymbol{x}^U$$
$$\mathcal{R}_1 : \text{counterclockwise vertices } \boldsymbol{x}_{P_i}, \boldsymbol{x}'', \boldsymbol{x}', \boldsymbol{x}^U$$
$$\mathcal{R}_2 : \text{counterclockwise vertices } \boldsymbol{x}_{P_i}, \boldsymbol{x}'', \boldsymbol{x}^L .$$

We can use the same argument if there is more than one vertex (i.e., more than $\boldsymbol{x}'$) of Ω_{goal} from $\boldsymbol{x}^L$ to $\boldsymbol{x}^U$ counterclockwise.

By Definition 4, $\mathcal{R}_0$ is a natural convex GCP for $\boldsymbol{x}_{P_i}$. Then, $\mathcal{R}_1$ is convex as 1) it is constructed by replacing the constraint by the line through $\boldsymbol{x}_{P_i}$ and $\boldsymbol{x}^L$ with the constraint by the line through $\boldsymbol{x}_{P_i}$ and $\boldsymbol{x}''$ and 2) the first two constraints in (15) ensure that

$$\theta^L \in D[\sigma(\boldsymbol{x}^U, \boldsymbol{x}_{P_i}), \sigma(\boldsymbol{x}_{P_i}, \boldsymbol{x}^L)] .$$

Also note that $\boldsymbol{x}_{P_i} \in \mathcal{R}_1$ and $\Omega_{\text{goal}} \subset \mathcal{R}_1$. In order to show that $\mathcal{R}_1$ is a convex GCP for $\boldsymbol{x}_{P_i}$, it remains to prove that $\mathcal{R}_1$ is obstacle-free. Since $\mathcal{R}_1 = \mathcal{R}_0 \cup \mathcal{R}_2$ and $\mathcal{R}_0$ is obstacle-free, the problem is reduced to proving that the orange region $\mathcal{R}_2$ is obstacle-free. Suppose that $\mathcal{R}_2$ is not obstacle-free. Then, we have that 1) either $\mathcal{R}_2$ contains at least one obstacle; 2) or there is an obstacle edge penetrating at least one of edges $\overline{\boldsymbol{x}''\boldsymbol{x}^L}$ and $\overline{\boldsymbol{x}''\boldsymbol{x}_{P_i}}$; 3) or mixture of 1) and 2). For the case 1), there must exist an obstacle vertex in $\mathcal{R}_2$ that has a strictly smaller value for (15), which contradicts with the fact that $\boldsymbol{y}^L$ is the first-visible obstacle vertex. For the case 2), if the obstacle edge only penetrates $\overline{\boldsymbol{x}''\boldsymbol{x}^L}$, then it goes back to case 1) as there will be at least one visible obstacle vertex in $\mathcal{R}_2$. If the obstacle edge penetrates $\overline{\boldsymbol{x}''\boldsymbol{x}_{P_i}}$, then $\boldsymbol{y}^L$ is not visible. For the case 3), it goes back to either 1) or 2). Moreover, $\mathcal{R}_2$ is obstacle-free even if three points $\boldsymbol{x}_{P_i}, \boldsymbol{x}^L$ and $\boldsymbol{x}'$ are collinear as we can extend $\overline{\boldsymbol{x}^U\boldsymbol{x}'}$ via $\boldsymbol{x}'$ and prove similarly. Hence, $\mathcal{R}_2$ is obstacle-free and thus $\mathcal{R}_1$ is a convex GCP for $\boldsymbol{x}_{P_i}$.

Then, for the part on θ^U, we define the following polygons:

$$\mathcal{R}_3 : \text{counterclockwise vertices } \boldsymbol{x}_{P_i}, \boldsymbol{x}^L, \boldsymbol{x}', \boldsymbol{x}^U, \boldsymbol{y}^U$$
$$\mathcal{R}_4 : \text{counterclockwise vertices } \boldsymbol{x}_{P_i}, \boldsymbol{x}'', \boldsymbol{x}', \boldsymbol{x}^U, \boldsymbol{y}^U .$$

By the similar analysis, we obtain that $\mathcal{R}_3$ is a convex GCP for $\boldsymbol{x}_{P_i}$. Since $|D[\theta^L, \theta^U]| \le \pi$, we have that $\mathcal{R}_4$ is a convex GCP for $\boldsymbol{x}_{P_i}$ where $D_{\mathcal{R}_4}(\boldsymbol{x}_{P_i}) = D[\theta^L, \theta^U]$.

Case 2: $|D[\theta^L, \theta^U]| > \pi$, shown in Fig. 7(b). We define the polygon $\mathcal{R}^5$ whose counterclockwise vertices are $\boldsymbol{x}_{P_i}$, $\boldsymbol{y}^L$ and $\boldsymbol{x}^L$. Following the same argument in the case 1, we obtain that $\mathcal{R}^3$ and $\mathcal{R}^5$ are convex GCPs for $\boldsymbol{x}_{P_i}$. Since $\mathcal{R}^5$ is obstacle free and $|D[\theta^L, \theta^U]| > \pi$, then by extending $\overline{\boldsymbol{y}^U \boldsymbol{x}_{P_i}}$ via $\boldsymbol{x}_{P_i}$ we can expand $\mathcal{R}_3$ and construct a convex GCP $\mathcal{R}_6$ for $\boldsymbol{x}_{P_i}$ such that $D_{\mathcal{R}_6}(\boldsymbol{x}_{P_i}) = D[\theta^U - \pi, \theta^U]$. Similarly, by expanding $\mathcal{R}_5$, we can construct a convex GCP $\mathcal{R}_7$ for $\boldsymbol{x}_{P_i}$ such that $D_{\mathcal{R}_7}(\boldsymbol{x}_{P_i}) = D[\theta^L, \theta^L + \pi]$, which completes the proof. $\square$

V. CLOSE-TO-GOAL PURSUIT WINNING II: NON-GOAL-VISIBLE CASE

In this section, we present the second case for the close-to-goal pursuit winning where the pursuers cannot see the whole goal region. We will construct the pursuit winning region and strategy based on the Euclidean shortest path, reachable region and wavefront in the presence of polygonal obstacles.

A. Euclidean shortest path, reachable region and wavefront

We first review three geometric concepts and then present two lemmas on the representations.

Definition 10 (Euclidean shortest path, [16]). *Given two points $\boldsymbol{x}_1, \boldsymbol{x}_2$ in Ω_{free}, a Euclidean shortest path (ESP) between them, denoted by $P_{\text{ESP}}(\boldsymbol{x}_1, \boldsymbol{x}_2)$, is an obstacle-free path of minimum total length connecting $\boldsymbol{x}_1$ and $\boldsymbol{x}_2$.*

Definition 11 (ESP reachable region). *For a point $\boldsymbol{x} \in \Omega_{\text{free}}$, the ESP reachable region from $\boldsymbol{x}$ in a distance $\ell \geq 0$, denoted by $\mathcal{R}_{\text{ESP}}(\boldsymbol{x}, \ell)$, consists of points in Ω_{free} whose ESP distance to $\boldsymbol{x}$ is less than or equal to ℓ.*

Definition 12 (Wavefront, [16]). *For a point $\boldsymbol{x} \in \Omega_{\text{free}}$, the wavefront from $\boldsymbol{x}$ in a distance $\ell \geq 0$, denoted by $W_{\text{ESP}}(\boldsymbol{x}, \ell)$ (may be empty), consists of points in Ω_{free} whose ESP distance to $\boldsymbol{x}$ is ℓ.*

For visualization, the ESP, ESP reachable region and wavefront are drawn in blue path in Fig. 8(a), grey region and its boundary in Fig. 8(b), respectively. Let $d_{\text{ESP}}(\boldsymbol{x}_1, \boldsymbol{x}_2)$ be the length of $P_{\text{ESP}}(\boldsymbol{x}_1, \boldsymbol{x}_2)$. If ESPs are not unique, $P_{\text{ESP}}(\boldsymbol{x}_1, \boldsymbol{x}_2)$ may refer to an arbitrary one. The next two lemmas show that the ESP and wavefront have finite representations.

Lemma 6 (ESP Representation, [16]). *An ESP $P_{\text{ESP}}(\boldsymbol{x}_1, \boldsymbol{x}_2)$ can be represented as an ordered set of obstacle vertices plus starting point $\boldsymbol{x}_1$ and ending point $\boldsymbol{x}_2$.*

Lemma 7 (Wavefront representation, [16]). *A nonempty wavefront $W_{\text{ESP}}(\boldsymbol{x}, \ell)$ can be represented as a set of disjoint paths (called wavelets) with an index set I, and each wavelet $k \in I$ is a circular arc centered on an obstacle vertex or $\boldsymbol{x}$.*

With the ordered set in Lemma 6, an ESP can be recovered by sequentially connecting the vertices in this set. By Lemma 7, each wavelet can be described by a tuple $(\boldsymbol{y}, \epsilon, \theta_1, \theta_2)$ which represents a circular arc centered at an obstacle vertex (or the start point) $\boldsymbol{y}$ with radius ϵ starting from angle θ_1 and ending at angle θ_2 counterclockwise. For instance, two adjacent wavelets (i.e., two red curves, which correspond to circular sectors with
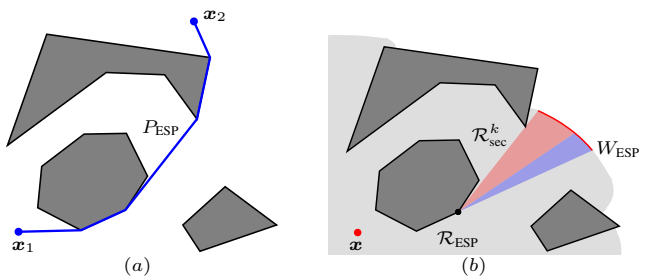

Fig. 8. Geometric concepts. (a) A (blue) Euclidean shortest path (ESP) P_{ESP} between $\boldsymbol{x}_1$ and $\boldsymbol{x}_2$. (b) The grey region $\mathcal{R}_{\text{ESP}}$ is the ESP reachable region from $\boldsymbol{x}$ in a given distance, and its boundary W_{ESP} is called wavefront. The wavefront W_{ESP} is a set of circular wavelets and each (red) wavelet induces a circular sector $\mathcal{R}_{\text{sec}}^k$ centered on an obstacle vertex or $\boldsymbol{x}$. The red and blue regions are two circular sectors centered on the same vertex induced by two adjacent wavelets, respectively. Notably, the division of W_{ESP} into wavelets is based on the ESP algorithm in [16].

different colors) are highlighted in Fig. 8(b). A wavefront is then constructed by connecting all adjacent wavelets (please refer to [16] for details). Notably, the division of W_{ESP} into wavelets here is based on the ESP algorithm in [16].

Remark 8. *In this paper, for a wavelet $(\boldsymbol{y}, \epsilon, \theta_1, \theta_2)$, if the angle difference from θ_1 to θ_2 in a counterclockwise direction is greater than π, we split this wavelet evenly into two shorter wavelets whose angle differences will be not more than π. Such a split can ensure each wavelet induces a convex circular sector (e.g., the red or blue region in Fig. 8(b)), which will be used to construct the pursuit winning region below.*

B. Non-goal-visible pursuit winning

Combing the ESP, reachable region, wavefront and the goal-visible pursuit winning in Section IV, we next construct the pursuit winning region and strategy for the pursuer who is not at a goal-visible point. The idea is to first steer the pursuer to a goal-visible point and then check if the pursuit winning can be guaranteed from this point via Theorem 2. We generalize the safe distance in order to check the condition (ii) in Theorem 2. Let $V_{\text{obs}}^{\text{gv}} \subset V_{\text{obs}}$ be the set of goal-visible obstacle vertices, for instance, green obstacle vertices in Fig. 9 are all goal-visible. First, we generalize the safe distance as follows.

Definition 13 (Anchored ESP-based safe distance). *For a state X_{ij} and a goal-visible obstacle vertex $\boldsymbol{s} \in V_{\text{obs}}^{\text{gv}}$, the anchored ESP-based safe distance $\varrho_A(X_{ij}, \boldsymbol{s})$ is defined as the optimal value of the problem*

$$
\begin{aligned}
\underset{\bar{\boldsymbol{x}}, \boldsymbol{x}, \boldsymbol{y} \in \mathbb{R}^2}{\text{minimize}} \quad & \|\boldsymbol{x} - \boldsymbol{y}\|_2 \\
\text{subject to} \quad & \bar{\boldsymbol{x}} \in \mathcal{R}_{\text{ESP}}(\boldsymbol{x}_{E_j}, d_{\text{ESP}}(\boldsymbol{x}_{P_i}, \boldsymbol{s})/\alpha_{ij}) \\
& f_{ij}(\boldsymbol{x}, \boldsymbol{s}, \bar{\boldsymbol{x}}) \geq 0, A_m \boldsymbol{y} + \boldsymbol{b}_m \geq 0, \forall m \in I_{\text{goal}}.
\end{aligned}
$$
(18)

Remark 9. *The anchored ESP-based safe distance $\varrho_A(X_{ij}, \boldsymbol{s})$ involves two stages as in Fig. 9: in the first stage, P_i moves to a goal-visible obstacle vertex $\boldsymbol{s}$ (called anchor point) along an ESP which takes the time $d_{\text{ESP}}(\boldsymbol{x}_{P_i}, \boldsymbol{s})/v_{P_i}$. The grey region is the ESP reachable region $\mathcal{R}_{\text{ESP}}(\boldsymbol{x}_{E_j}, d_{\text{ESP}}(\boldsymbol{x}_{P_i}, \boldsymbol{s})/\alpha_{ij})$ from $\boldsymbol{x}_{E_j}$ in this duration. In the second stage, $\varrho_A(X_{ij}, \boldsymbol{s})$ is defined as the minimal safe distance when P_i is at $\boldsymbol{s}$ while E_j can*
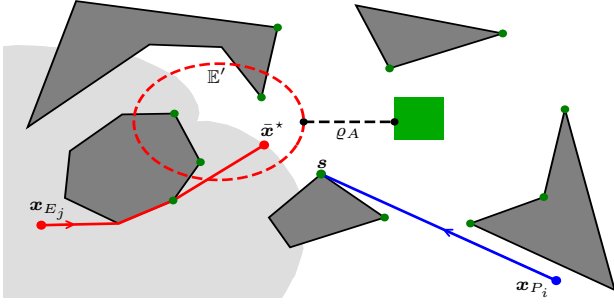
Fig. 9. Non-goal-visible pursuit winning. All goal-visible obstacle vertices $V_{\text{obs}}^{\text{gv}}$ are in green. If P_i is not goal-visible and there exists $s \in V_{\text{obs}}^{\text{gv}}$ such that the anchored ESP-based safe distance ϱ_A is non-negative, then P_i guarantees to win against E_j. The distance ϱ_A anchored at s is computed as follows. In the first stage, P_i moves to s along an (blue) ESP, and the grey region is the ESP reachable region from x_{E_j} in this duration. In the second stage, ϱ_A is defined as the minimal safe distance when P_i is at s and E_j is at any point (say $\bar{x}^\star$ achieves the minimum) in the grey region. The pursuit winning strategy is to first move along the ESP to s and then adopting the goal-visible pursuit winning strategy.

be any point in the grey region. In the figure, $\bar{x}^\star$ achieves the minimal safe distance.

Since $\mathcal{R}_{\text{ESP}}(x_{E_j}, d_{\text{ESP}}(x_{P_i}, s)/\alpha_{ij})$ is generally non-convex due to the presence of obstacles, computing the anchored ESP-based safe distance involves solving the nonlinear optimization problem (18). We next present an approximate, efficient solution to the problem (18), thus providing a sufficient condition for the non-negative anchored ESP-based safe distance. Recall that the angle difference for any wavelet is not more than π by Remark 8. The following concept is required.

Definition 14 (Circular sectors for a wavefront). *For a wavefront $W_{\text{ESP}}(x, \ell)$ with an index set I, let $\mathcal{R}_{\text{sec}}^k$ be the circular sector (e.g., red region in Fig. 8(b)) formed by a wavelet $k \in I$, represented by $(y, \epsilon, \theta_1, \theta_2)$, and its center y, i.e.,*

$$\mathcal{R}_{\text{sec}}^k = \{z \in \mathbb{R}^2 \mid \|z - y\|_2 \leq \epsilon, [-\sin\theta_1, \cos\theta_1]^\top z \geq 0$$
$$[-\sin\theta_2, \cos\theta_2]^\top z \leq 0\}.$$

Then, $\mathcal{R}_{\text{sec}} = \{\mathcal{R}_{\text{sec}}^k \mid k \in I\}$ is called the circular sectors *for $W_{\text{ESP}}(x, \ell)$.*

Lemma 8 (Non-negative anchored ESP-based safe distance). *For a state X_{ij} and a goal-visible obstacle vertex $s \in V_{\text{obs}}^{\text{gv}}$, let I and $\mathcal{R}_{\text{sec}}$ be the index set and circular sectors for the wavefront $W_{\text{ESP}}(x_{E_j}, d_{\text{ESP}}(x_{P_i}, s)/\alpha_{ij})$, respectively. If*

1) $\alpha_{ij} d_{\text{ESP}}(x_{E_j}, x) \geq d_{\text{ESP}}(x_{P_i}, s)$ for all $x \in V_{\text{goal}}$;
2) $\min_{k \in I} J_k^\star \geq 0$;

where let $d_k = \max_{z \in \mathcal{R}_{\text{sec}}^k} \|z - s\|_2$ for a wavelet $k \in I$ and $J_k^\star$ is the optimal value to the convex optimization problem

$$\begin{aligned}
\underset{\bar{x}, x, y \in \mathbb{R}^2}{\text{minimize}} \quad & \|x - y\|_2 \\
\text{subject to} \quad & \bar{x} \in \mathcal{R}_{\text{sec}}^k, \; A_m y + b_m \geq 0, \forall m \in I_{\text{goal}} \\
& \|x - \bar{x}\|_2 \leq (d_k - r_i)/(\alpha_{ij} - 1) \\
& \|x - s\|_2 \leq (\alpha_{ij} d_k - r_i)/(\alpha_{ij} - 1)
\end{aligned} \quad (19)$$

then $\varrho_A(X_{ij}, s) \geq 0$.

Proof. The condition 1) indicates that E_j has not yet reached any vertex of Ω_{goal} when P_i reaches s. This implies that for

each circular sector $\mathcal{R}_{\text{sec}}^k \in \mathcal{R}_{\text{sec}}$, the associated center's ESP distance to x_{E_j} is not more than $d_{\text{ESP}}(x_{P_i}, s)/\alpha_{ij}$.

Since $\mathcal{R}_{\text{sec}}^k$ is a convex set and the other constraints in (19) are convex, then (19) is a convex optimization problem.

Using Definitions 11, 12 and 14 and Lemma 7, we have $\cup_{k \in I} \mathcal{R}_{\text{sec}}^k \subset \mathcal{R}_{\text{ESP}}(x_{E_j}, d_{\text{ESP}}(x_{P_i}, s)/\alpha_{ij})$. Therefore, Definition 13 implies that the lemma holds if the last two constraints in (19) are looser than the constraint $f_{ij}(x, s, \bar{x}) \geq 0$ in (18).

We relax $f_{ij}(x, s, \bar{x}) \geq 0$ into two looser constraints:

$$\|x - \bar{x}\|_2 + \|\bar{x} - s\|_2 - \alpha_{ij}\|x - \bar{x}\|_2 - r_i \geq 0 \Rightarrow$$
$$\|x - \bar{x}\|_2 \leq (\|\bar{x} - s\|_2 - r_i)/(\alpha_{ij} - 1) \leq (d_k - r_i)/(\alpha_{ij} - 1)$$

and

$$\|x - s\|_2 - \alpha_{ij}(\|x - s\|_2 - \|s - \bar{x}\|_2) - r_i \geq 0 \Rightarrow$$
$$\|x - s\|_2 \leq \frac{\alpha_{ij}\|s - \bar{x}\|_2 - r_i}{\alpha_{ij} - 1} \leq \frac{\alpha_{ij} d_k - r_i}{\alpha_{ij} - 1}$$

which thus completes the proof. $\qquad \square$

Utilising all these ESP-based concepts, we next present the pursuit winning region and strategy for the non-goal-visible case of the close-to-goal pursuit winning, illustrated in Fig. 9.

Theorem 4 (Non-goal-visible pursuit winning). *At time t, if the positions X_{ij} of P_i and E_j are such that*

1) x_{P_i} *is not goal-visible;*
2) *there exists at least one goal-visible obstacle vertex $s \in V_{\text{obs}}^{\text{gv}}$ such that the anchored ESP-based safe distance is non-negative, i.e., $\varrho_A(X_{ij}, s) \geq 0$;*

then P_i can guarantee to win against E_j, regardless of E_j's strategy, by using the pursuit strategy that computes $u_{P_i}(\tau)$ for $\tau \geq t$ as follows:

$$\begin{cases}
\text{Along } P_{\text{ESP}}(x_{P_i}(t), s) & \text{if } t \leq \tau \leq t + d_{\text{ESP}}(x_{P_i}(t), s)/v_{P_i} \\
(9) & \text{if } \tau > t + d_{\text{ESP}}(x_{P_i}(t), s)/v_{P_i}.
\end{cases} \quad (20)$$

Proof. A goal-visible obstacle vertex $s \in V_{\text{obs}}^{\text{gv}}$ exists such that $\varrho_A(X_{ij}(t), s) \geq 0$. Then, as Remark 9 states, P_i can reach the vertex s along the ESP $P_{\text{ESP}}(x_{P_i}(t), s)$ which takes the time $d_{\text{ESP}}(x_{P_i}(t), s)/v_{P_i}$. The safe distance is non-negative when P_i reaches s, regardless of E_j' strategy. Thus, since s is goal-visible, then by Theorem 2 the strategy (9) can ensure P_i's winning against E_j. $\qquad \square$

VI. MULTIPLAYER PURSUIT STRATEGY

In this section, we propose a multiplayer pursuit strategy by fusing the subgame outcomes in Sections III, IV and V with hierarchical optimal task allocation to ensure a lower bound on the number of defeated evaders and improve the bound continually. Before that, we first present an evasion winning region and strategy which can conversely help the pursuit team to distribute its team members to the evaders more efficiently.

A. Evasion winning

Based on the ESP, we construct an evasion winning region and strategy which will be used in the following matchings.

Lemma 9 (ESP-based evasion winning). *If the positions X_{ij} of P_i and E_j are such that there exists $\boldsymbol{x} \in \Omega_{\text{goal}}$ satisfying*

$$d_{\text{ESP}}(\boldsymbol{x}_{P_i}, \boldsymbol{x}) - r_i > \alpha_{ij} d_{\text{ESP}}(\boldsymbol{x}_{E_j}, \boldsymbol{x}) \tag{21}$$

then E_j can guarantee to reach Ω_{goal} before being captured by P_i by moving along $P_{\text{ESP}}(\boldsymbol{x}_{E_j}, \boldsymbol{x})$, regardless of P_i' strategy.

Proof. Suppose that at time t, the positions of P_i and E_j are X_{ij}. The conclusion follows if we can prove that the distance between two players is always greater than r_i when E_j moves along $P_{\text{ESP}}(\boldsymbol{x}_{E_j}(t), \boldsymbol{x})$. It implies that $\|\boldsymbol{x}_{P_i}(\tau) - \boldsymbol{x}_{E_j}(\tau)\|_2 > r_i$ for all $t \le \tau \le t + d_{\text{ESP}}(\boldsymbol{x}_{E_j}(t), \boldsymbol{x})/v_{E_j}$. For simplicity, we let $d_{\text{ESP}}^P = d_{\text{ESP}}(\boldsymbol{x}_{P_i}(t), \boldsymbol{x})$ and $d_{\text{ESP}}^E = d_{\text{ESP}}(\boldsymbol{x}_{E_j}(t), \boldsymbol{x})$.

Suppose that there exists a pursuit strategy $\boldsymbol{u}'_{P_i}$ such that E_j is captured by P_i, i.e., $\|\boldsymbol{x}_{P_i}(\tau') - \boldsymbol{x}_{E_j}(\tau')\|_2 \le r_i$, at some time $t \le \tau' \le d_{\text{ESP}}^E/v_{E_j} + t$. We can construct an obstacle-free path $\mathcal{P}'$ along which P_i can reach $\boldsymbol{x}$: first, move to $\boldsymbol{x}_{P_i}(\tau')$ under $\boldsymbol{u}'_{P_i}$; then, move to $\boldsymbol{x}_{E_j}(\tau')$ directly (recall that this path is obstacle-free due to the visual capture condition); finally, move along part of $P_{\text{ESP}}(\boldsymbol{x}_{E_j}(t), \boldsymbol{x})$ to reach $\boldsymbol{x}$ as $\boldsymbol{x}_{E_j}(\tau')$ is on the path $P_{\text{ESP}}(\boldsymbol{x}_{E_j}(t), \boldsymbol{x})$. Let t' be the time of P_i reaching $\boldsymbol{x}$ along the path $\mathcal{P}'$. Then we have $t' \le \tau' + (r_i + d_{\text{ESP}}^E - v_{E_j}(\tau' - t))/v_{P_i}$. Thus, the length of $\mathcal{P}'$, denoted by $d(\mathcal{P}')$, satisfies

$$\begin{aligned}
d(\mathcal{P}') - d_{\text{ESP}}^P &= v_{P_i}(t' - t) - d_{\text{ESP}}^P \\
&\le v_{P_i}(\tau' - t) + r_i + d_{\text{ESP}}^E - v_{E_j}(\tau' - t) - d_{\text{ESP}}^P \\
&< (1 - 1/\alpha_{ij})v_{P_i}(\tau' - t) + r_i + (d_{\text{ESP}}^P - r_i)/\alpha_{ij} - d_{\text{ESP}}^P \\
&= (1 - 1/\alpha_{ij})(v_{P_i}(\tau' - t) + r_i - d_{\text{ESP}}^P) \\
&\le (1 - 1/\alpha_{ij})(v_{P_i} d_{\text{ESP}}^E/v_{E_j} + r_i - d_{\text{ESP}}^P) < 0,
\end{aligned}$$

where the second and fourth inequalities are due to (21), which is a contradiction as d_{ESP}^P is the ESP from $\boldsymbol{x}_{P_i}$ and $\boldsymbol{x}$. $\square$

As a sufficient and efficient method, we practically check the evasion winning condition (21) over finitely many critical points in Ω_{goal}, for instance, the vertices of Ω_{goal}.

B. Multiplayer onsite and close-to-goal pursuit strategy

We next present the *multiplayer onsite and close-to-goal (MOCG) pursuit strategy* in Algorithm 1. In each iteration, the strategy first generates a hierarchical task allocation between pursuit coalitions and evaders to maximize the number of defeated evaders (a lower bound). Then, the strategy computes the pursuit strategies that can ensure the lower bound. The task allocation is dynamic and will change over time (therefore, the pursuit strategies may also change), if a new task allocation guaranteeing to defeat more evaders is generated as the game evolves. The hierarchical task allocation involves four matchings which are generated sequentially at each iteration.

Capture matching. Firstly, we generate a capture matching in which each matched evader can be defeated by the assigned pursuer(s). By Remarks 3 and 6 and Theorem 4, the capture matching is simplified as we only need to consider all pursuit

---

Algorithm 1 MOCG pursuit strategy

Initialize: $\{\boldsymbol{x}_{P_i}^0\}_{P_i \in \mathscr{P}}$, $\{\boldsymbol{x}_{E_j}^0\}_{E_j \in \mathscr{E}}$

1: $\boldsymbol{x}_{P_i} \leftarrow \boldsymbol{x}_{P_i}^0$, $\boldsymbol{x}_{E_j} \leftarrow \boldsymbol{x}_{E_j}^0$ for all $P_i \in \mathscr{P}$ and $E_j \in \mathscr{E}$
2: $\mathcal{V}_P \leftarrow [\mathscr{P}]^2$, $\mathcal{V}_E \leftarrow \mathscr{E}$
3: $\mathscr{E}_{\text{capture}} \leftarrow \emptyset$, $M_{\text{defeat}} \leftarrow \emptyset$
4: **repeat**
5:     **for** $P_i \in \mathscr{P}$, $E_j \in \mathcal{V}_E$ **do**
6:         $T_{ij} \leftarrow$ Check_pursuit_winning(X_{ij})
7:         Add e_{ij} to $\mathcal{E}$ if $T_{ij} \ge 1$
8:     **for** $P_c \in \mathcal{V}_P$, $E_j \in \mathcal{V}_E$ **do**
9:         **if** $|c| = 2$ and $e_{ij} \notin \mathcal{E}$ for all $i \in c$ **then**
10:             $T_{cj} \leftarrow$ Check_pursuit_winning(X_{cj})
11:             Add e_{cj} to $\mathcal{E}$ if $T_{cj} = 2$
12:     $M_1^\star \leftarrow$ solve the BIP (22) for graph $(\mathcal{V}_P \cup \mathcal{V}_E, \mathcal{E})$
13:     $M_{\text{defeat}} \leftarrow M_1^\star$ if $|M_1^\star| > M_{\text{defeat}}$
14:     **for** $e_{cj} \in M_{\text{defeat}}$ **do**
15:         $\boldsymbol{u}_{P_i} \leftarrow$ Lemma 1 agst. E_j if $T_{ij} = 1$ ($c = \{i\}$)
16:         $\boldsymbol{u}_{P_i} \leftarrow$ (9) agst. E_j if $T_{cj} = 2$ for all $i \in c$
17:         $\boldsymbol{u}_{P_i} \leftarrow$ (20) agst. E_j if $T_{ij} = 3$ ($c = \{i\}$)
18:     **for** unassigned $P_i \in \mathscr{P}$ **do**
19:         $\boldsymbol{u}_{P_i} \leftarrow$ Lemma 1 agst. an $E_j \in \mathcal{V}_E$ if $T_{ij} = 1$
20:     $\bar{\mathcal{V}}_P, \bar{\mathcal{V}}_E \leftarrow$ all unmatched $P_i \in \mathscr{P}$ and $E_j \in \mathcal{V}_E$
21:     **for** $P_i \in \bar{\mathcal{V}}_P$, $E_j \in \bar{\mathcal{V}}_E$ **do**
22:         Add e_{ij} to $\bar{\mathcal{E}}$ if (21) does not hold
23:     $M_2^\star \leftarrow$ a maximum matching for graph $(\bar{\mathcal{V}}_P \cup \bar{\mathcal{V}}_E, \bar{\mathcal{E}})$
24:     $\boldsymbol{u}_{P_i} \leftarrow$ Definition 15 agst. E_j for all $e_{ij} \in M_2^\star$
25:     **for** unassigned $P_i \in \mathscr{P}$ **do**
26:         $\boldsymbol{u}_{P_i} \leftarrow$ Definition 15 agst. closest E_j
27:     Adopt any strategy for $E_j \in \mathcal{V}_E$
28:     Update $\boldsymbol{x}_{P_i}, \boldsymbol{x}_{E_j}$ with a time step Δ
29:     $\mathscr{E}_{\text{capture}} \leftarrow \mathscr{E}_{\text{capture}} \cup \{\text{captured evader(s) in } \mathcal{V}_E\}$
30:     Remove captured/arrival evaders from $\mathcal{V}_E$ and M_{defeat}
31: **until** $\mathcal{V}_E = \emptyset$

Algorithm 2 Check_pursuit_winning(X_{cj})

1: $T_{cj} \leftarrow 0$
2: **if** X_{cj} satisfies (5) for all $i \in c$ **then**
3:     $T_{cj} \leftarrow 1$ ▷ Onsite pursuit winning
4: **else if** X_{cj} meets conditions in Theorem 2 **then**
5:     $T_{cj} \leftarrow 2$ ▷ Visible-goal pursuit winning
6: **else if** $|c| = 1$ & X_{cj} meets conditions in Theorem 4 **then**
7:     $T_{cj} \leftarrow 3$ ▷ Non-visible-goal pursuit winning
8: **return** T_{cj}

---

coalitions of size no more than two. Let $\mathcal{G} = (\mathcal{V}_P \cup \mathcal{V}_E, \mathcal{E})$ be an undirected bipartite graph with two vertex sets $\mathcal{V}_P$ and $\mathcal{V}_E$, and a set of edges $\mathcal{E}$. In our problem, $\mathcal{V}_P$ is the set of all nonempty pursuit coalitions of size less than or equal to two, and $\mathcal{V}_E$ the set of evaders. The edge connecting vertex $P_c \in \mathcal{V}_P$ and vertex $E_j \in \mathcal{V}_E$ is denoted by e_{cj}. For a state X_{cj}, we check the pursuit winning via Check_pursuit_winning(X_{cj}) (Algorithm 2). We add e_{cj} into $\mathcal{E}$ if and only if the returned value satisfies $T_{cj} \ge 1$, that is, P_c guarantees to win against E_j through the onsite ($T_{cj} = 1$), goal-visible ($T_{cj} = 2$) or

non-goal-visible ($T_{cj} = 3$) pursuit winnings. Let $\mathcal{C} = (\mathcal{E}, \bar{\mathcal{E}})$ be a conflict graph of $\mathcal{G}$, where each vertex in $\mathcal{C}$ corresponds uniquely to an edge in $\mathcal{G}$. An edge $\bar{e} \in \bar{\mathcal{E}}$ if and only if two vertexes (two edges in $\mathcal{G}$) connected by $\bar{e}$ involve at least one common pursuer.

The problem of maximizing the number of defeated evaders can be formulated as a binary integer program (BIP):

$$\begin{aligned}
\underset{a_{cj}, a_{pq} \in \{0,1\}}{\text{maximize}} \quad & \sum_{e_{cj} \in \mathcal{E}} a_{cj} \\
\text{subject to} \quad & \sum_{P_c \in \mathcal{V}_P} a_{cj} \leq 1, \quad \forall E_j \in \mathcal{V}_E \\
& \sum_{E_j \in \mathcal{V}_E} a_{cj} \leq 1, \quad \forall P_c \in \mathcal{V}_P \\
& a_{cj} + a_{pq} \leq 1, \quad \forall (e_{cj}, e_{pq}) \in \bar{\mathcal{E}}
\end{aligned} \quad (22)$$

where $a_{cj} = 1$ means the allocation of P_c to capture E_j, and $a_{cj} = 0$ means no assignment. Let $\boldsymbol{a}^\star$ be an optimal solution to (22). Then, we obtain a maximum matching $M_1^\star \subset \mathcal{E}$ of $\mathcal{G}$ subject to the constraint $\mathcal{C}$, where $e_{cj} \in M_1^\star$ if and only if $a_{cj}^\star = 1$. For each assignment $(P_c, E_j) \in M_1^\star$, the pursuer(s) in P_c adopts the strategy in Lemma 2, Theorems 2 or 4 depending on the value of T_{cj} to capture E_j (lines 5-17).

Enhanced matching. We then generate an enhanced matching to improve the performance of the onsite matchings in $M_1^\star$. As Remark 3 indicates that, the more pursuers that can ensure the onsite pursuit winning against an evader are tasked to the evader, the smaller or equal region in which the evader will be captured. Therefore, we assign each unassigned pursuer to an evader it can win against via the onsite winning (lines 18-19).

Non-dominated matching. We next generate a non-dominated matching in which no pursuer is assigned to an evader that it cannot win against. For the remaining unmatched pursuers $\bar{\mathcal{V}}_P$ and evaders $\bar{\mathcal{V}}_E$, let $\bar{\mathcal{G}} = (\bar{\mathcal{V}}_P \cup \bar{\mathcal{V}}_E, \bar{\mathcal{E}})$ be an undirected bipartite graph, where $e_{ij} \in \bar{\mathcal{E}}$ if and only if E_j cannot ensure the evasion winning in Lemma 9. A non-dominated matching $M_2^\star$ is then a maximum bipartite matching of $\bar{\mathcal{G}}$ which can be computed in polynomial time (e.g., via maximum network flow [10]). Each pursuer adopts the following ESP-pure strategy to pursue the matched evader (lines 20-24).

Definition 15 (ESP-pure pursuit strategy). *For the positions X_{ij} of P_i and E_j, if $\boldsymbol{u}_{P_i}$ is along the ESP $P_{\text{ESP}}(\boldsymbol{x}_{P_i}, \boldsymbol{x}_{E_j})$ at $\boldsymbol{x}_{P_i}$, then $\boldsymbol{u}_{P_i}$ is called the ESP-pure pursuit strategy.*

Closest matching. We finally generate a closest matching for the remaining unassigned pursuers. If these pursuers exist, then it means that either 1) all evaders have been matched or 2) the remaining evaders can win against them. Therefore, a closest matching is as follows: each remaining unassigned pursuer pursues the closest unmatched evader if present and the closest evader otherwise, via the ESP-pure pursuit strategy (lines 25-26).

We have the following guarantee on the number of defeated evaders with the MOCG pursuit strategy.

Theorem 5 (Increasing lower bound for guaranteed defeated evaders). *Using the MOCG pursuit strategy, the pursuit team $\mathscr{P}$ guarantees to win against at least $|\mathscr{C}_{\text{capture}}| + |M_{\text{defeat}}|$ evaders simultaneously at each iteration, regardless of the evasion team $\mathscr{E}$'s strategy. Moreover, $|\mathscr{C}_{\text{capture}}| + |M_{\text{defeat}}|$ is increasing with iterations.*

Proof. The conclusion directly follows from Theorems 1, 2 and 4, and the fact that the matching will change only if more evaders can be defeated in the new matching. $\square$

VII. SIMULATIONS

In order to illustrate the MOCG pursuit strategy, we run the multiplayer reach-avoid differential games in various scenarios with different obstacle shapes and distributions, team sizes and initial configurations. We use the first-visible obstacle vertices to construct convex GCPs (see Theorem 3) if necessary. In all scenarios, the strategies of the evaders are generated randomly which are unknown to the pursuers. The games in all scenarios take less than one minute as the pursuit winning regions and strategies have closed forms or require solving simple convex optimization problems.

Case 1: onsite pursuit winning. Consider three pursuers P_1, P_2, P_3 and one evader E_1 in Fig. 10(1a). The initial positions of each pursuer and E_1 satisfy (5), as they are close and there is no obstacle nearby. Thus, by Theorem 1, each pursuer can ensure the onsite pursuit winning against E_1 individually via the strategy in Lemma 1, i.e., capture E_1 in the corresponding dotted expanded Apollonius circle in a finite time, regardless of E_1's strategy. Furthermore, Lemma 2 demonstrates that E_1 will be captured in the intersection of three regions bounded by the expanded Apollonius circles. In this case, P_1 captures E_1 at the yellow star.

Case 2: goal-visible pursuit winning. Consider two pursuers P_1, P_2 and one evader E_1 in Fig. 10(2a). Their initial positions do not satisfy (5) but conditions in Theorem 2. In Fig. 10(2a), two pursuers are goal-visible with the orange direction ranges. The safe distance is positive as the red closest point in the evasion region to the goal region is outside the goal region. Thus, two pursuers can ensure the goal-visible pursuit winning via the strategy (9), regardless of E_1's strategy. In the snapshot of Fig. 10(2b), two pursuers are heading towards the closest point as this point is in their direction ranges. The snapshot of Fig. 10(2c) shows that P_1 captures E_1 at the yellow star.

Case 3: non-goal-visible pursuit winning. Consider two pursuers P_1, P_2 and two evaders E_1, E_2 in Fig. 10(3a). Their initial positions do not satisfy (5) and conditions in Theorem 2. In Fig. 10(3a), two pursuers are not goal-visible and all goal-visible obstacle vertices are in green. P_1 and E_1 (also P_2 and E_2) meet the conditions in Theorem 4 initially. Thus, P_1 (resp., P_2) ensures the non-goal-visible pursuit winning against E_1 (resp., E_2) via the strategy (20), despite E_1's (resp., E_2's) strategy. The goal-visible obstacle vertices that two pursuers are heading for are marked as larger green vertices. In the snapshot of Fig. 10(3b), P_2 has passed the vertex and become goal-visible with the orange direction range, while P_1 has not yet. In the snapshot of Fig. 10(3c), P_1 and P_2 are both goal-visible. In the snapshot of Fig. 10(3d), two pursuers capture the evaders using the onsite pursuit winning strategy as in the final period, they are close with no obstacles nearby.
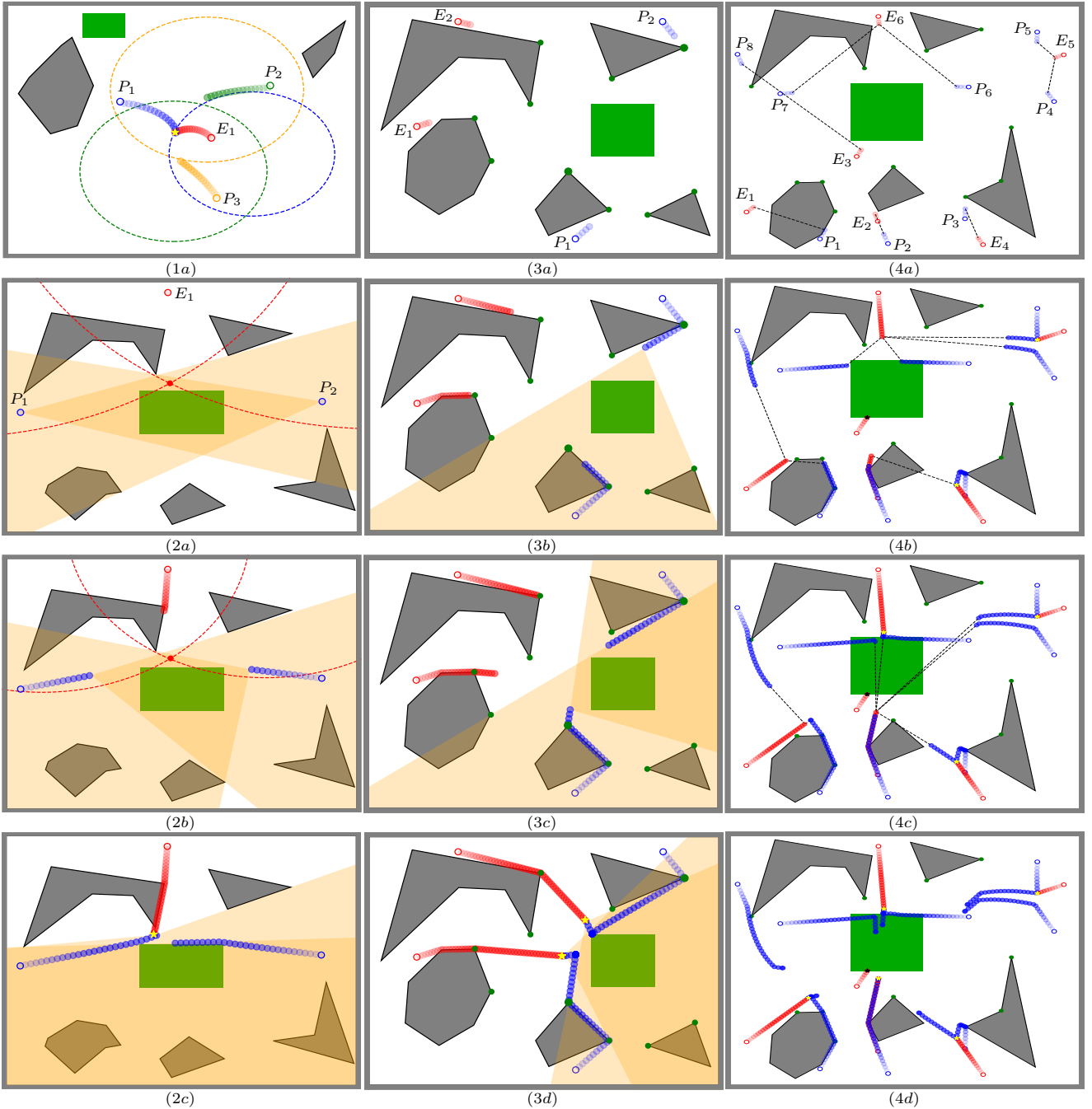
Fig. 10. Four simulations with the MOCG pursuit strategy. (1a) Onsite pursuit winning for three pursuers and one evader. (2a)-(2c) Goal-visible pursuit winning for two pursuers and one evader. (3a)-(3d) Non-goal-visible pursuit winning for two pursuers and two evaders. (4a)-(4d) Three pursuit winnings for eight pursuers and six evaders.

Case 4: Three pursuit winnings. Consider eight pursuers P_i ($i = 1, \ldots, 8$) and six evaders E_j ($j = 1, \ldots, 6$) in Fig. 10(4a). The MOCG pursuit strategy initially generates six matchings indicated by dotted lines: two two-to-one and four one-to-one matching pairs. The capture matchings include: 1) P_4 ensures the onsite pursuit winning against E_5; 2) P_6 and P_7 ensure the goal-visible pursuit winning against E_6; 3) P_1 (resp., P_3) ensures the non-goal-visible winning against E_1 (resp., E_4). The enhanced matching is P_5 against E_5 via the onsite pursuit winning. There is one closest matching between P_8 and E_3. Therefore, the MOCG pursuit strategy can guarantee to win

against four evaders initially. In the snapshot of Fig. 10(4b), E_3 is able to reach the goal region, while E_4 and E_5 have been captured respectively by P_3 and P_5 who continue to capture other evaders. In the snapshot of Fig. 10(4c), the pursuers still guarantee to defeat four evaders where three have been captured and one (i.e., E_1) is being pursued. In the snapshot of Fig. 10(4d), the pursuers are able to capture five evaders, which demonstrates that the MOCG pursuit strategy can achieve an increasing number of defeated evaders as the game evolves.

VIII. Conclusion

We presented the MOCG pursuit strategy for multiplayer reach-avoid differential games in polygonal environments with general polygonal obstacles. This strategy provides a lower bound on the number of defeated evaders and continually improve the lower bound if a task allocation that can win against more evaders is found as the game evolves. This strategy does not require the state space discretization as in many HJ-based approaches and is computationally efficient. This is because all pursuit winning regions and strategies involved either have closed forms or are computed by solving simple convex optimization problems. The three proposed winnings cover three common scenarios. The onsite pursuit winning corresponds to the scenario where the pursuers are close to the evader with no obstacles nearby. The goal-visible case for the close-to-goal pursuit winning corresponds to the scenario where the pursuers can visibly see the whole goal region, while the non-goal-visible case corresponds to the scenario where the visibility fails. The three main employed concepts, expanded Apollonius circles, convex GCPs and ESPs, show that computational geometry methods are powerful in solving games with obstacles. The hierarchical task assignment prioritizes the number of defeated evaders and is complete as it generates the tasks for all pursuers. Future work will involve distributed games, games with limited visible areas and more complicated reconnaissance games with obstacles [20].

References

[1] D. R. Anthony, D. P. Nguyen, D. Fridovich-Keil, and J. F. Fisac. Back to the future: Efficient, time-consistent solutions in reach-avoid games. In *2022 International Conference on Robotics and Automation (ICRA)*, pages 6830–6836, 2022.

[2] S. Bajaj, S. D. Bopardikar, A. Von Moll, E. Torng, and D. W. Casbeer. Perimeter defense using a turret with finite range and startup time. In *2023 American Control Conference (ACC)*, pages 3350–3355, 2023.

[3] T. Başar and G. J. Olsder. *Dynamic Noncooperative Game Theory*. 2 edition, 1999.

[4] P. Cardaliaguet. A differential game with two players and one target. *SIAM Journal on Control and Optimization*, 34(4):1441–1460, 1996.

[5] M. Chen, S. L. Herbert, M. S. Vashishtha, S. Bansal, and C. J. Tomlin. Decomposition of reachable sets and tubes for a class of nonlinear systems. *IEEE Transactions on Automatic Control*, 63(11):3675–3688, 2018.

[6] M. Chen, Z. Zhou, and C. J. Tomlin. Multiplayer reach-avoid games via pairwise outcomes. *IEEE Transactions on Automatic Control*, 62(3):1451–1457, 2017.

[7] X. Chen and J. Yu. Reach-avoid games with two heterogeneous defenders and one attacker. *IET Control Theory & Applications*, 16(3):301–317, 2022.

[8] V. S. Chipade and D. Panagou. Multiagent planning and control for swarm herding in 2-D obstacle environments under bounded inputs. *IEEE Transactions on Robotics*, 37(6):1956–1972, 2021.

[9] M. Dorothy, D. Maity, D. Shishika, and A. Von Moll. One Apollonius circle is enough for many pursuit-evasion games. *Automatica*, 163:111587, 2024.

[10] L. R. Ford Jr and D. R. Fulkerson. *Flows in networks*, volume 56. Princeton university press, 2015.

[11] H. Fu and H. H-T Liu. Justification of the geometric solution of a target defense game with faster defenders and a convex target area using the HJI equation. *Automatica*, 149:110811, 2023.

[12] E. Garcia, D. W. Casbeer, and M. Pachter. Optimal strategies for a class of multi-player reach-avoid differential games in 3D space. *IEEE Robotics and Automation Letters*, 5(3):4257–4264, 2020.

[13] E. Garcia, D. W. Casbeer, A. V. Moll, and M. Pachter. Multiple pursuer multiple evader differential games. *IEEE Transactions on Automatic Control*, 66(5):2345–2350, 2020.

[14] W. M. Getz and M. Pachter. Two-target pursuit-evasion differential games in the plane. *Journal of Optimization Theory and Applications*, 34(3):383–403, 1981.

[15] S. Y. Hayoun and T. Shima. On guaranteeing point capture in linear n-on-1 endgame interception engagements with bounded controls. *Automatica*, 85:122–128, 2017.

[16] J. Hershberger and S. Suri. An optimal algorithm for Euclidean shortest paths in the plane. *SIAM Journal on Computing*, 28(6):2215–2256, 1999.

[17] R. Isaacs. *Differential Games*. New York: Wiley, 1965.

[18] N. T. Kokolakis and K. G. Vamvoudakis. Safety-aware pursuit-evasion games in unknown environments using Gaussian processes and finite-time convergent reinforcement learning. *IEEE Transactions on Neural Networks and Learning Systems*, pages 1–14, 2022.

[19] E. S. Lee, L. Zhou, A. Ribeiro, and V. Kumar. Graph neural networks for decentralized multi-agent perimeter defense. *Frontiers in Control Engineering*, 4:1104745, 2023.

[20] Y. Lee and E. Bakolas. Two-player reconnaissance game with half-planar target and retreat regions. In *2023 American Control Conference (ACC)*, pages 3344–3349, 2023.

[21] Y. Li, J. He, C. Chen, and X. Guan. Intelligent physical attack against mobile robots with obstacle-avoidance. *IEEE Transactions on Robotics*, 39(1):253–272, 2022.

[22] L. Liang, F. Deng, M. Lu, and J. Chen. Analysis of role switch for cooperative target defense differential game. *IEEE Transactions on Automatic Control*, 66(2):902–909, 2021.

[23] E. Lozano, I. Becerra, U. Ruiz, L. Bravo, and R. Murrieta-Cid. A visibility-based pursuit-evasion game between two nonholonomic robots in environments with obstacles. *Autonomous Robots*, 46(2):349–371, 2022.

[24] K. Margellos and J. Lygeros. Hamilton–Jacobi formulation for reach–avoid differential games. *IEEE Transactions on Automatic Control*, 56(8):1849–1861, 2011.

[25] I. M. Mitchell. *Application of level set methods to control and reachability problems in continuous and hybrid systems*. Stanford University, 2002.

[26] I. M. Mitchell, A. M. Bayen, and C. J. Tomlin. A time-dependent Hamilton-Jacobi formulation of reachable sets for continuous dynamic games. *IEEE Transactions on Automatic Control*, 50(7):947–957, 2005.

[27] J. Mohanan, N. Kothuri, and B. Bhikkaji. The target guarding problem: A real time solution for noise corrupted measurements. *European Journal of Control*, 54:111–118, 2020.

[28] D. W. Oyler, P. T. Kabamba, and A. R. Girard. Pursuit–evasion games in the presence of obstacles. *Automatica*, 65:1–11, 2016.

[29] P. Rivera, M. Kobilarov, and Y. Diaz-Mercado. Pursuer coordination against a fast evader via coverage control. *IEEE Transactions on Automatic Control*, pages 1–6, 2023.

[30] J. Selvakumar and E. Bakolas. Feedback strategies for a reach-avoid game with a single evader and multiple pursuers. *IEEE transactions on cybernetics*, 51(2):696–707, 2019.

[31] J. Selvakumar and E. Bakolas. Min–max Q-learning for multi-player pursuit-evasion games. *Neurocomputing*, 475:1–14, 2022.

[32] L. Shamgah, T. G. Tadewos, A. A. R. Newaz, A. Karimoddini, and A. C. Esterline. Reactive symbolic planning and control in dynamic adversarial environments. *IEEE Transactions on Automatic Control*, 68(6):3409–3424, 2023.

[33] D. Shishika and V. Kumar. A review of multi agent perimeter defense games. In *International Conference on Decision and Game Theory for Security*, pages 472–485, 2020.

[34] D. Shishika, D. Maity, and M. Dorothy. Partial information target defense game. In *2021 IEEE International Conference on Robotics and Automation (ICRA)*, pages 8111–8117, 2021.

[35] J. Silveira, K. Cabral, C. Rabbath, and S. Givigi. Deep reinforcement learning solution of reach-avoid games with superior evader in the context of unmanned aerial systems. In *2023 International Conference on Unmanned Aircraft Systems (ICUAS)*, pages 911–918, 2023.

[36] A. V. Moll, M. Pachter, D. Shishika, and Z. Fuchs. Circular target defense differential games. *IEEE Transactions on Automatic Control*, 68(7):4065–4078, 2023.

[37] S. Velhal, S. Sundaram, and N. Sundararajan. A decentralized multirobot spatiotemporal multitask assignment approach for perimeter defense. *IEEE Transactions on Robotics*, 38(5):3085–3096, 2022.

[38] P. Wasz, M. Pachter, and K. Pham. Two-an-one pursuit with a non-zero capture radius. In *2019 27th Mediterranean Conference on Control and Automation (MED)*, pages 577–582, 2019.

[39] R. Yan, R. Deng, X. Duan, Z. Shi, and Y. Zhong. Multiplayer reach-avoid differential games with simple motions: A review. *Frontiers in Control Engineering*, 3:1093186, 2023.

[40] R. Yan, X. Duan, Z. Shi, Y. Zhong, and F. Bullo. Matching-based capture strategies for 3D heterogeneous multiplayer reach-avoid differential games. *Automatica*, 140:110207, 2022.

[41] R. Yan, Z. Shi, and Y. Zhong. Reach-avoid games with two defenders and one attacker: An analytical approach. *IEEE Transactions on Cybernetics*, 49(3):1035–1046, 2019.

[42] R. Yan, Z. Shi, and Y. Zhong. Task assignment for multiplayer reach-avoid games in convex domains via analytical barriers. *IEEE Transactions on Robotics*, 36(1):107–124, 2020.

[43] R. Yan, Z. Shi, and Y. Zhong. Optimal strategies for the lifeline differential game with limited lifetime. *International Journal of Control*, 94(8):2238–2251, 2021.

[44] Z. Zhou, J. Huang, J. Xu, and Y. Tang. Two-phase jointly optimal strategies and winning regions of the capture-the-flag game. In *47th Annual Conference of the IEEE Industrial Electronics Society*, pages 1–6, 2021.

[45] Z. Zhou, J. R. Shewchuk, D. Stipanović, H. Huang, and C. J. Tomlin. Smarter lions: Efficient cooperative pursuit in general bounded arenas. *SIAM Journal on Control and Optimization*, 58(2):1229–1256, 2020.

[46] Z. Zhou, R. Takei, H. Huang, and C. J. Tomlin. A general, open-loop formulation for reach-avoid games. In *2012 IEEE 51st IEEE Conference on Decision and Control (CDC)*, pages 6501–6506, 2012.

[47] Z. Zhou, W. Zhang, J. Ding, H. Huang, D. M. Stipanović, and C. J. Tomlin. Cooperative pursuit with Voronoi partitions. *Automatica*, 72:64–72, 2016.

[48] R. Zou and S. Bhattacharya. On optimal pursuit trajectories for visibility-based target-tracking game. *IEEE Transactions on Robotics*, 35(2):449–465, 2018.